Geomagnetically Induced Currents and Harmonic Distortion: Storm-time Observations from New Zealand

Craig J. Rodger

Department of Physics, University of Otago, Dunedin, New Zealand

Mark A. Clilverd

British Antarctic Survey (NERC), Cambridge, United Kingdom

Daniel H. Mac Manus

Department of Physics, University of Otago, Dunedin, New Zealand

Ian Martin and Michael Dalzell

Transpower New Zealand Limited, New Zealand

James B. Brundell, Tim Divett, and Neil R. Thomson

Department of Physics, University of Otago, Dunedin, New Zealand

Tanja Petersen

GNS Science, New Zealand

Yuki Obana

Osaka Electro-Communication University, Neyagawa, Osaka, Japan

Neville R. Watson

College of Engineering, University of Canterbury, Christchurch, New Zealand

Main point # 1: Harmonic distortion measurements made at 126 locations in New Zealand are used to locate stressed transformers during geomagnetic storms.

Main point # 2: Geomagnetically induced current effects on transformers can be identified through commonly-measured even harmonic distortion data.

Main point # 3: Even harmonic distortion is observed in unexpectedly low latitude locations during the 06-09 September 2017 geomagnetic storm period.

Abstract. Large geomagnetic storms are a known space weather hazard to power transmission networks due to the effects of Geomagnetically Induced Currents (GICs). However, research in this area has been hampered by a lack of GIC observations. Previous studies have noted that New Zealand is unusually fortunate in having a comparatively dense, high quality, set of GIC measurements, spanning >60 transformers in >20 substations. However, due to operational reasons these observations are clustered in the mid and lower South Island. In this paper we analyze space weather-induced GIC impact patterns over the entire country by using a different set of sensors that monitor levels of harmonic distortion, with even and odd harmonics measured separately. GICs lead to half cycle transformer saturation and is one of the few ways in which even harmonics are produced in a well run power transmission network. We make use of harmonic distortion measurements at 377 circuit breakers made at 126 separate locations. Focusing on the intense geomagnetic storm activity during 06 to 09 September 2017, we show how the even harmonic distortion observations provide a useful new picture of GIC-stressed transformers. These observations demonstrate how GIC effects can be monitored by using even harmonic distortion in locations where no GIC measurements are present (for example, the most of the North Island). We understand harmonic distortion measurements are fairly common in electrical networks and could provide a new tool for Space Weather researchers.

1. Introduction

There is a rising global recognition of Space Weather as a hazard to our deeply technologically-connected society. An example is the recent report from UN Committee on the Peaceful Uses of Outer Space [*United Nations*, 2017]. They noted that "The largest potential socioeconomic impacts arise from space weather driven geomagnetically induced currents in electrical power networks". An extreme storm is likely to produce a collapse of the electrical power grid with damage to the infrastructure and loss of service [e.g., *JASON*, 2011; *Baker et al.*, 2008; *Oughton et al.*, 2017]. Reliable electricity supply is the lifeblood of any modern nation. The cost of damage to network components is small compared to the knock-on consequences of electrical outages to essential services, businesses and households. It should be noted that Geomagnetically Induced Currents (GICs) are one of a wide range of Space Weather impacts which occur during extreme storms, some of which could be described as "extraordinary" [*Knipp et al.*, 2016; *Love and Coïsson*, 2016; *Knipp et al.*, 2018].

There are multiple ways by which Geomagnetically Induced Currents can adversely affect electrical power infrastructure through physical damage or disruption to supply [e.g., *Samuelsson*, 2013; *Boteler*, 2015]. One of the ways to disruption comes from the production of harmonic distortion to the alternating current (AC) waveform generated by saturated transformers. The GIC, being quasi-direct current (DC), produces half-cycle saturation in transformers with consequent excessive heating of the transformers and increased audible noise. In addition, saturated transformers dissipate large quantities of power. These in turn cause voltage dips, changes in power flow, possible system frequency shifts and incorrect operation of protective relays [*EPRI*, 1983].

The most commonly invoked example of GIC effects is the blackout of March 1989 [*Bolduc*, 2002; *Béland and Small*, 2004; *Guillon et al.*, 2016], when the Hydro-Québec's (TransÉnergie) electric transmission system collapsed in 92 seconds. Protective relays were tripped, the grid collapsed [*Guillon et al.*, 2016], and about 9 million people were left without electricity [*Bolduc*, 2002]. The cause was the geomagnetic disturbance (GMD) which occurred in the North American sector on 13 March 1989 at 2:44 am eastern standard time (7:44 UT). In roughly 1.5 minutes, the Hydro-Québec's electric transmission system went from stable operation to total collapse, with the tripping of static VAR compensators, power oscillation, voltage collapse, and the separation of parts of the transmission system (see the detailed description in *Béland and Small* [2004] and *Guillon et al.* [2016], and the recent report on the space weather causes of this event [*Boteler*, 2019]). The 7:44 UT GMD was caused by a magnetospheric substorm causing surface level magnetic fields to change rapidly. This GMD came after the commencement of a sudden storm (1:30 UT) which did not produce significant power network effects, as well as two subsequent substorms (3 UT and 6 UT), the second of which created GIC strong enough to cause voltage fluctuations. In the case of the 6 UT substorm Hydro-Québec system operators had sufficient time to undertake switching, allowing for network voltage control [*Guillon et al.*, 2016]. This was not possible during the third, even more intense 7:44 UT substorm. This substorm-induced GIC saturated many power transformers, which in turn drew more reactive power and also became strong sources of harmonics. The extra reactive power could have been supplied by static VAR compensators (SVCs) units located in the network to regulate the grid voltage. However the available SVCs tripped off due to the high harmonic currents, with seven large SVCs lost in one minute, triggering the system collapse. It is clear that GIC-produced-harmonic-distortion was the primary cause of the Hydro Quebec blackout in 1989 [*Guillon et al.*, 2016].

In the aftermath of the March 1989 blackout, Hydro-Québec introduced multiple monitoring systems to assist the system operators. These include: real-time monitoring and control centre reporting of voltage harmonics at 9 substations, real-time monitoring and control centre reporting of even harmonic distortion at 4 substations, and offline monitoring of voltage and current harmonics plus DC GIC observations at 5 substations [*Guillon et al.*, 2016].

New Zealand is one of the few countries that has already experienced direct transformer damage from a large geomagnetic storm. On 6 November 2001 at 14:53 alarms from monitors across the South Island were received by the network operator, Transpower New Zealand Ltd. Simultaneously a static VAR compensator at Christchurch city tripped along with a transformer feeding Dunedin city. The transformer at Dunedin/Halfway Bush (HWB T4) failed within one minute of the storm start [*Béland and Small*, 2004; *Marshall et al.*, 2012; *Mac Manus et al.*, 2017]. In recent years this has stimulated a focus on space weather impacts on the New Zealand electrical network, exploiting the significant quantity of DC GIC observations available in parts of that country [*Mac Manus et al.*, 2017]. Those observations are available in the system operations control room, and operational procedures have been developed to try to mitigate GIC impact during a GMD [*Transpower*, 2015].

The extensive New Zealand GIC dataset has been used to show that the rate of change of the *H*-component (*H'*) of the local magnetic field is the best correlated driver of observed GIC magnitude but not for every storm in every location [*Mac Manus et al.*, 2017]. Investigations of likely extreme GIC magnitude within New Zealand estimated a peak GIC that could occur in a 100 year return period at a particular transformer near Christchurch as ~155–605 A [*Rodger et al.*, 2017]. A different approach based on magnetic field transfer functions found similarly large peak GIC magnitude at multiple New Zealand locations [*Ingham et al.*, 2017]. However, *Divett et al.* [2018] modeling responses to a given GIC event for different

transformers at the same substation, found variations of up to a factor of 9, depending on the electrical connections.

In New Zealand the majority of the DC observations are clustered in the middle and southern part of the South Island, for operational reasons (as outlined in section 3 below). Due to the shape and geographic orientation of New Zealand, there is a strong tendency for electric fields to orient northeast-southwest [*Divett et al.*, 2017], parallel to the main structure of the country along which many main transmission lines run. This contributes to a high potential for GIC over most of the country and especially the South Island [*Divett et al.*, 2017].

Most recently, a unique set of observations from Halfway Bush, New Zealand, were used to examine the behavior of harmonic distortion during a series of GMD from 7–8 September 2017 [*Clilverd et al.*, 2018]. This study combined local and nearby magnetic field variation observations, GIC measurements, and harmonic distortion observations made both at low time resolution by Transpower and very high time resolution using a co-located VLF wideband radio receiver. These measurements showed increases in even-order harmonics once GIC levels measured at the monitored transformers at the Halfway Bush substation exceeded 15 A, in one case for >30 min. In contrast, no evidence of harmonic production was found during the much shorter periods of impulsive magnetic field changes generated from solar wind shocks, even though they produced very large peak GIC (~35 A) for a short duration. This suggests the transformer was less "stressed" than for long lasting but smaller averaged magnitude GIC levels [*Clilverd et al.*, 2018].

As noted above, harmonic distortion observations provide a different way to look at the space weather impact on power transmission networks. It is common for space weather

researchers to use modeling approaches to investigate GIC across networks. However, typically these modeling efforts rely on significant assumptions, and their validation may be based on limited GIC observations. A different approach, therefore, is to look for evidence of stressed transformers using network wide harmonic observations. Until now there have been limited simultaneous harmonic distortion experimental observations and GIC measurements presented in the literature. One reason for this may be that most countries have limited GIC measurements available to link to the harmonic distortion observations. Another reason is that network operators in some nations may be unwilling to release one or both of these datasets to researchers. New Zealand is unusually well positioned to investigate the occurrence of GIC in a mid-latitude country as there are comparatively large quantities of measurements available to our space weather research team. In this study we build on the earlier work of *Clilverd et al.* [2018], and primarily focus on the GMDs which occurred during 7–8 September 2017. While that study concentrated in and around the Halfway Bush substation in Dunedin, we make use of the larger GIC dataset which primarily covers the mid- and lower South Island. We complement those observations with harmonic distortion measurements which span both North and South Islands. The harmonic distortion observations provide new insights into the occurrence of GIC leading to transformer saturation.

2. Asymmetric Saturation and Even Harmonic Production

As noted above, harmonic distortion played a central role in the Hydro-Québec blackout. It is an important precursor to supply disruption and/or transformer damage, and is now actively monitored in Hydro-Québec due to the space weather hazard. It is instructive to consider how GIC causes asymmetric saturation and harmonic production. In addition to the text below, we direct the interested reader to *EPRI* [2014] and *Arrillaga and Watson* [2003].

When a transformer is subjected to higher than rated AC voltage or lower than rated frequency, the magnetic flux during the peak parts of the sinusoidal cycle may exceed the capabilities of the transformer core and cause it to go into saturation. With AC over-excitation, the magnetic flux peaks exceed both the positive and negative saturation thresholds, resulting in both positive and negative “spikes” of exciting current. This produces only odd-order harmonic components and is called symmetric saturation. While not desirable, this sort of saturation leading to odd harmonics is a standard consideration for electrical engineers. Power engineers typically design systems to avoid the production and impact of odd-order harmonics.

In contrast, the transformer core flux will have an offset if there is a DC component in one of the transformer windings. In this case the transformer core saturates in only one direction, such that the exciting current spike appears only once per cycle for only one polarity. This type of saturation is termed asymmetric saturation or "half-cycle" saturation. As should be clear, GIC provides the DC offset described above, and such GIC is a source of asymmetric transformer saturation. It is important to note that because of the asymmetric nature of the current spikes, half-cycle saturation results in even- and odd-order harmonic components [e.g., *Boteler et al.*, 1989; *Walling et al.*, 1991]. It is common in electrical engineering papers on GIC to mention the existence of both even and odd harmonics in this situation, but without commenting on how unusual even-order harmonic production is in a typical electrical transmission network. We believe this is because the importance is obvious to the power engineering readers of these papers but is likely less so to space weather researchers. We hence emphasize that GIC leading to asymmetric transformer saturation is one of the few ways to produce even harmonics, and as such even-order harmonic measurements should be a very valuable route to study space weather impacts on power networks.

3. Experimental Datasets

3.1 New Zealand GIC Observations

A detailed description of the New Zealand GIC measurements in the South Island has been previously reported [*Mac Manus et al.*, 2017]. The following section is a brief summary, and the reader is directed to the earlier study for a more complete explanation.

Transpower New Zealand Limited has measured DC currents in multiple South Island transformers using Hall effect current transducers (Liaisons Electroniques-Mécaniques (LEM) model LT 500 or LT 505, with about half of each in use, and a mix of -S and -T subtypes for both model cases). The primary purpose for the DC observations is monitoring stray currents when the high voltage DC link between the South and North Islands operates in single wire earth return mode or with unbalanced currents on the conductors. This type of operation is common for the New Zealand HVDC link. For our purposes the LEM-provided DC measurements need to be corrected to remove the stray currents as described by *Mac Manus et al.* [2017], leaving only GIC. During GMD the typical LEM sampling rate is one measurement every 4 s.

Recently, we have become aware that the archived DC current dataset is in fact slightly larger than was described in *Mac Manus et al.* [2017] and hence we update the overview details in the current study. The locations of the substations with the original monitoring equipment are shown as yellow stars in the left panel of Figure 1. Table 1 indicates how the number of transformers and substations monitored has varied with time. Over the years the DC monitoring has expanded from 13 substations and 36 transformers (November 2001) to 22 substations and 60 transformers (from November 2018), with the later part of that growth

being in the lower South Island with a space weather focus. Different colored stars show the new substations monitored in the left hand panel of Figure 1. Note from Table 1 that the number of transformers monitored has both increased and decreased through new DC monitoring deployments and decommissionings/faults, and peaked in early 2015. Obviously the number of operational DC monitors has recently shrunk. Following the new space weather activity Transpower is currently looking to repair all faulty DC monitors, and install new monitors into at least one additional substation in the near future.

The GIC-sensing DC monitors provide real-time observations to the network operator control rooms. At this time they are the primary indicator through which the operators would invoke a GIC mitigation strategy [*Transpower*, 2015] aimed at decreasing the total current into each transformer by removing redundant transmission lines from operation. At this time the protocol is focused only on the lower South Island. However, there is evidence that GMD may produce significant GIC further equatorwards, where no DC monitors are located. For example the GIC modeling reported by *Divett et al.* [2018] showed that significant GIC is expected to occur at the top of the South Island.

3.2 New Zealand Harmonic Distortion Observations

The earlier Halfway Bush case study into the 7-8 September 2017 GMD used Total Harmonic Distortion (THD) measurements made of the voltage at circuit breaker CB532 inside the Halfway Bush substation in Dunedin. In the current study we expand the analysis to examine all voltage input harmonic distortion observations made across New Zealand in the same time period. Harmonic distortion observations are made at every substation in New Zealand using Schneider PowerLogic ION8800 meters, which provide harmonic reporting up to the 63rd harmonic on both voltage and current inputs. The meters are capable of providing total, even-order, and odd-order harmonic recording. In Transpower's case the summed total,

even, and odd-order harmonic distortion percentages are archived from each meter on each of the three phases with a 10 min time resolution. Note that the timestamp for the 10 min resolution THD observations is for the end of the window; in subsequent snapshot maps we will specify both the start and stop times of this window for clarity. In the current study we focus only on the percentage distortion of the sum of all even-order harmonics monitored on the circuit breaker voltage input, which we term the even-THD.

During the GMD of 7-8 September 2017 harmonic monitoring was undertaken at 133 substations (84 in the North Island and 49 in the South Island), with metering on a total of 391 individual circuit breakers (257 in the North Island and 134 in the South Island). Unfortunately, in some locations the data quality is not good, and we have to remove the data for a small number of circuit breakers (~3.5%) from our analysis. After this removal we have available even-THD from 126 substations (79 in the North Island and 47 in the South Island), including 377 circuit breakers (245 in the North Island and 132 in the South Island). The distribution of available even-THD measurements is shown in the right hand panel of Figure 1; this figure demonstrates the even-THD observations cover all the Transpower primary transmission network (a nation-wide grid map is available from *Transpower* [2019]). A number of locations of interest which are discussed later in this text are shown in red in the right hand panel of Figure 1.

At this time the harmonic distortion observations are not fed to the network operators in real time; the measurements are archived and are available for post-event analysis.

It is important to note that voltage harmonic distortion observed at a given monitoring location may not be locally generated. A saturated transformer will produce current harmonics which can be measured as voltage harmonics at a connected but separate

277 substation. In contrast, current harmonic distortion provide a direct indication as to where the
278 harmonics are originating from. As such, current harmonic distortion measurements should
279 provide space weather researchers with a more direct indication of the location of stressed
280 transformers. Unfortunately, the Transpower harmonic distortion observations from the
281 current input do not discriminate between even and odd, providing only the sum of both. As
282 shown in *Clilverd et al.* [2018], while even harmonics are directly related to transformer
283 saturation, odd harmonic occurrence is less clear. We have found the combination of both,
284 i.e., the total of both even and odd harmonic distortion, does not respond in a useful way
285 during space weather events. Thus in this study we limit ourselves to the use of the even
286 order voltage harmonic distortion observations, i.e., even-THD. Researchers who can access
287 even order current harmonic distortion measurements should be able to investigate this
288 directly, hopefully leading to additional insight. We hope to be able to undertake such studies
289 through dedicated future campaigns.
290
291 **3.3 New Zealand Magnetometer Observations**
292 Building on the earlier New Zealand GIC studies, and in particular *Clilverd et al.* [2018], we
293 make use of magnetic field observations from multiple locations. The locations of the
294 magnetometers are shown in the maps where the data is used (in particular Figures 4-8). The
295 magnetometers are:
296 1. The Eyrewell (EYR) magnetometer operated by GNS Science, New Zealand which is part
297 of INTERMAGNET (http://www.intermagnet.org/). A detailed description of the
298 construction of EYR 1 minute averages of the horizontal component of the magnetic field is
299 given in *Mac Manus et al.* [2017].
300 2. Magnetometers at Middlemarch and Te Wharau operated by Osaka Electro-
301 Communication University, Japan, forming the CRUX array [*Obana et al.*, 2015]. The Te
302 Wharau and Middlemarch variometers measure magnetic field on a fixed orientation

determined at the time of installation. This is aligned so that the primary axis is pointing towards magnetic north (h), secondary axis is pointing towards magnetic east (e), and the tertiary axis vertically down (Z). To convert from this heZ coordinate system to HDZ we have used the 2015v2 World Magnetic Model [*Chulliat et al.*, 2019] as a baseline for the conversion.

3. A magnetometer at Swampy Summit near Dunedin. This instrument has been described by *Clilverd et al.* [2018].

At this time none of the magnetometer observations are fed to the system operations control rooms. The Swampy Summit magnetometer is available in near real time, and discussions have taken place around providing the EYR magnetic data to the control rooms in near-real time, as well as archiving the magnetic field data inside the main Transpower monitoring dataset.

4. Summary of 7-8 September 2017 GMD

The time period from 04-11 September 2017 interval included a number of different space weather forcing events that produced impacts on ground- and space-based instrumentation. Space Weather published a special issue on this event (available from https://agupubs.onlinelibrary.wiley.com/doi/toc/10.1002/(ISSN)1542-7390.SW-SEPT2017), which provides a large amount of background on the activity and impacts. The event period included X-class solar flares, a coronal mass ejection, high speed solar wind streams, a solar proton event, and a ground level event. The impacts included HF radio blackouts which disrupted emergency communication, Global Navigation Satellite Systems signal interferences, plasma bubble occurrence, and enhanced GIC. For the current study we focus on the geomagnetic storms of 7-8 September 2017, the same time period examined by

Clilverd et al. [2018]. The upper panel of Figure 2 shows the magnitude of the rate of change of the horizontal magnetic field (|*H'*|) observed by the EYR magnetometer. Following *Clilverd et al.* [2018], we highlight four distinct peaks in the EYR |*H'*| observations, as labelled red dashed lines in this panel. These four are at the following times: (1) 23:48 UT 06-Sep-2017, (2) 08:56 UT 07-Sep-2017, (3) 23:02 UT 07-Sep-2017, (4) 12:50 UT 08-Sep-2017. The four events correspond to: 1. Sudden Commencement due to the arrival of a shock in the solar wind, 2. a small substorm, 3. second sudden commencement solar wind shock arrival, and 4. storm period with strong negative deviation of the interplanetary magnetic field (IMF) component *Bz*.

In this study we focus primarily on the period at, and following, event 3 (22:00 UT on 07 September to 03:30 UT on 08 September 2017) and event 4 (12:00 to 13:00 UT on 08 September 2017). We choose to focus on these time periods as they include disturbed *H'* and were associated with GIC and even-THD at the Halfway Bush substation in Dunedin [*Clilverd et al.*, 2018]. In the present study we will examine the wider pattern in THD across New Zealand during these events, but first we remind the reader of the most salient results of the earlier study for these periods and the Halfway Bush, Dunedin, case study from Clilverd and coauthors.

Clilverd et al. [2018] reported that the Sudden Commencement at 23:02 UT on 07-Sep-2017 produced a short lived peak in GIC at Halfway Bush transformer number 4 (HWB T4), reaching ~34 A but lasting only a few minutes. This short peak was not linked to harmonic distortion seen in the high time resolution wideband VLF data, or the Transpower-provided even-THD 10 min-resolution measurements. We term this time period event 3a. *Clilverd et al.* [2018] also report that from 01:00 to 02:00 UT the GIC measured at HWB T4 shows enhanced GIC, exceeding >15 A for about 5 minutes at about 01:45 UT (see Figure 5 of that

study). We term this time period event 3b, and have marked it in our Figure 2 (middle panel). We note it was associated with clear and long-lasting increases in harmonic distortion, despite being much lower total GIC magnitude than event 3a. This event is likely to be associated with sudden changes in solar wind pressure caused by rapid density variations, and was described as a substorm by *Dimmock et al.* [2019].

In our study we also focus on event 4, which was driven by severe geomagnetic storming linked to strongly negative IMF B_z and high solar wind speeds, a large substorm enhancing currents locally, and the arrival of the CME ejecta enhancing magnetospheric currents globally [*Dimmock et al.*, 2019]. During this event HWB transformer T4 experienced long lasting GIC, with >15 A occurring for ~30 minutes and peaking at ~49 A [*Clilverd et al.*, Fig. 5, 2018], and associated harmonic distortion *Clilverd et al.*, Figures 6, 8, and 9, 2018]. The EYR $|H'|$ is shown in the lower panel of Figure 2.

5. Even-THD observations

5.1 Halfway Bush substation

As noted above, the Halfway Bush substation is located in the city of Dunedin, the location of which is marked in Figure 1. This substation has 5 different circuit breakers which have harmonic distortion monitors: CB0232, CB0292, CB0532, CB2542, and CB2582. The top panel of Figure 3 shows the Halfway Bush single line diagram with the voltage connections for the HWB substation. In this panel 3 of the 5 circuit breakers are marked. CB292 and CB232 are connected to the same 33kV bus, and so only the first of these are plotted. CB2582 and CB2542 are also on the same bus, so again, only one is plotted. The lower 4 panels of this figure show the percentage even-THD for each these circuit breakers, as labelled, as well as the combination of all the observations from the substation combined (i.e.,

all 5 monitored circuit breakers). As expected, the time variation for the measurements at CB292 and CB232 are essentially identical, as is also the case for CB2582 and CB2542. Because of this the measurements from the extra CB232 and CB2542 are not plotted. The red vertical lines in the lower 4 panels of Figure 3 correspond to the $|H'|$ peaks shown in the upper panel of Figure 2.

Each of the even-THD panels include the 3 separate phases (A, B, and C), and the mean of all 3 phases for that circuit breaker, the latter in black. The time behavior of the even-THD is very similar across the five circuit breakers, although not identical. Circuit Breakers CB0232 and CB0292, located on the left hand side of the electrical line diagram, display more variability than seen for the other 3 Circuit Breakers, found on the right hand side of the electrical line diagram, with extra spikes not seen in the other 3 CB panels. It is also clear that the first two circuit breakers mentioned respond at the times of the magnetic field changes we have termed Events 1, 3 and 4, while the later 3 only respond to Events 3 and 4. Finally the magnitude of the even-THD response for the first two circuit breakers is noticeably smaller than the last three; in the case of CB0232 and CB0292 the peak even-THD, which is associated with event period 4, is ~0.45%, whereas for CB0532, CB2542, and CB2582 the peak value is ~0.9%.

It is likely the nature of the transformers in the Halfway Bush substation, plus their electrical connections, can explain the approximate factor of two seen in THD magnitude between the two sets of circuit breakers. At the Halfway Bush substation, GIC will impact only T4 and T6. These two transformers have star connected high voltage windings which allow GIC to flow from the electrical earth into the windings. The other transformers present have delta connected high voltage windings and star connected low voltage windings. Delta connections do not have an earth connection so GIC cannot flow. Observational experience has shown

that we can ignore GIC impacts from transformers earthed on the low voltage side [e.g., *NERC*, 2013], such as these. This is because low voltage networks have relatively high resistances and short lengths compared to the high-voltage transmission lines meaning less GIC, and finally that low voltage windings have fewer turns so a given GIC causes less flux in the transformer. In Halfway Bush one can see from the upper panel of Figure 3 that CB0532 is on the 110 kV bus directly connected to T6. One can expect this circuit breaker to be more affected than CB0292, as the THD will need to propagate to them through T5, which will produce attenuation. This could explain why CB2582 has higher levels than CB0292. The former of these will get harmonics from the 110 kV bus while the latter will get harmonics from the 220 kV bus. In addition there are two transformers linking the 110 kV bus to the 33 kV bus and only one transformer linking the 220 kV bus to the 33 kV bus

The lower right hand panel of Figure 3 shows the combined mean of all 15 observations, i.e., the mean of the 3 phases at each of the 5 circuit breakers, combined into a single time-varying mean. We will take this to represent the time-varying summary even-THD value for the HWB substation, and follow the same practice for each sub-station with THD observations we have available. We undertake this combination to bring the New Zealand-wide even-THD dataset down to manageable proportions, from 1026 values at each 10 min interval (i.e., 3 phases and 342 circuit breakers) down to 126, one for each substation.

5.2 New Zealand Wide THD observations

We now examine the New Zealand-wide variation in even-THD observations using the large, and spatially comprehensive THD dataset. We focus in particular on Event periods 3 and 4, as they were earlier shown to have significant even-THD levels in Dunedin. We contrast the THD observations with those from the New Zealand GIC dataset. In order to produce a 'like with like' comparison, we average the GIC measurements to 10 min time

resolution, as the format of the THD observations. Where there is more than one GIC measurement in a substation (i.e., from multiple monitored transformers), our GIC-THD comparison maps will present the mean of all the GIC measurements in that substation, following the THD approach outlined above.

For this paper, we have produced a series of snapshot figures for different times of interest. These are supported by a movie available in the supplementary material.

Quiet Time example: We start by considering a quiet time period, to show the appearance for background conditions. This is shown in Figure 4, and is for the 10 min window from 21:50-22:00 UT on 7 September 2017; that is 1 hour before the time of the 2nd sudden commencement. This is not a totally quiet period, but is only very weakly disturbed, with the EYR-observed $|H'|$ ranging from 0-2 nT/min at 1 min resolution. When averaged over 10 min, as the GIC and THD data are in Figure 4, the $|H'|$ value at EYR is 0.9 nT/min. The left hand panel shows a map of the GIC observation magnitudes, with a red cross showing the location of the available GIC measurements. A blue ring around each cross would show the magnitude of the average GIC at each substation for this time period. Only the two Dunedin substations, Halfway Bush and South Dunedin, show any indication of non-negligible GIC magnitudes in this plot, with 1.4 A and 1 A, respectively. Previous studies have shown that the Dunedin substations have considerably higher GIC than many other New Zealand locations [*Rodger et al.*, 2017], consistent with the small but just-observable GIC for this very weakly disturbed time period.

The right hand map in Figure 4 shows the even-THD percentage at the same time period. Due to the large number of THD-locations (126 monitored sites) we do not show a cross for each location in this map. The values shown are very small; the largest, at Hokitika on the

West Coast of the South Island is 0.07%, and only 5 sites have values above 0.05%. The mean value across the country is 0.01%. Also shown in Figure 4 are the locations of the 4 magnetometer sites, shown by magenta squares, with the location named on the far left of each locations. To the left of the magnetometer locations, near 174.1ºE is a graphical indication of the absolute *H′* value at each of the magnetometer sites as shown by horizontal purple bars.

We do not suggest Figure 4 is particularly insightful in itself. We have included it both to present the format for the THD-GIC maps we will show below, and also to provide the reader with a comparison between quiet conditions and the highly disturbed periods which follow.

Event 3a: We now consider Event 3a, the second sudden commencement shown in Figure 2. This large but short-lived |*H′*| GMD was triggered by a solar wind shock seen at L1 at 22.38 UT that then arrived at Earth at 23:02 UT. The GIC-THD comparison for this time period is shown in Figure 5. The two upper panels report the peak 4 s resolution GIC magnitudes that occur during the *H′* peak. We express this through both a geospatial map and also a bar chart, to better demonstrate the GIC values and their spatial variation. The same format has earlier been used for GMD on 6 November 2001 [*Mac Manus et al.*, Fig. 5, 2017], and 2 October 2013 [*Mac Manus et al.*, Fig. 7, 2017]. In the upper two panels a green cross indicates a transformer for which no GIC data is currently available, but for which GIC data has been present for some time periods previously. For the right hand panel the letter "N" indicates transformers with installed Neutral Earthing Resistors.

The upper two panels of the plot show the different GIC magnitudes between different transformers in the same substation, and between different substations. In this case the differences between transformers in the same substation is not as dramatic as reported by

Divett et al. [2018], as many of the transformers reported in that study as having large modeled GIC did not have operational GIC-logging for the 7-8 September 2017 series of GMD. The largest GIC are seen at the Dunedin transformers at Halfway Bush, the nearby South Dunedin, and also Invercargill at the bottom of the South Island.

The lower two panels of Figure 5 present the 10-min average per substation GIC magnitude, as well as that for even-THD percentage, both shown in the same format as Figure 4. While the peak GIC magnitudes are large at the second sudden commencement time period, as seen in the upper panels, but plots of the GIC (not shown) show that they are fairly short-lived. When averaged over 10 min the high GIC peaks at Halfway Bush and South Dunedin have values of only ~6-7 A across the time window 23:00-23:10 UT. The only other location in the lower left hand panel which appears to show signs of significant GIC in this time window is Roxburgh, inland from Dunedin. This substation has one transformer monitored, which experiences a peak GIC of ~9 A during the sudden commencement. However, shortly after this there is a large data gap for this location including the decrease in GIC to much smaller levels, artificially boosting the mean value for the GIC data which does exist inside this 10 min period. The mean for all locations of the GIC observed across the 10min period is 1.4 A.

The lower right hand panel shows the even-THD voltage harmonic distortion. This panel presents THD data for the same time period as was shown for GIC in the lower left hand panel. The THD panel also shows a graphical indication of magnetometer $|H'|$ values for each magnetometer location through the use of horizontal purple bars as in Figure 4. For the sudden impulse these values are fairly large, despite being averaged over 10 min. For this sudden impulse time window the variation in $|H'|$ across the magnetometers is small, ranging from 9.9 nT/min at Swampy (near Dunedin) to 6.6 nT/min at Te Wharau in the lower North

Island. The largest even-THD observed is 0.21 % at Black Point substation, shown on the figure. The mean value across the country is ~0.03%, i.e., only 3 times the quiet time mean value, suggesting low-levels of GIC-stressed transformers in this 10 min time period. It is clear from Figure 5 that the sudden impulse may produce significant GIC for short time periods, but it is not sufficiently sustained to produce significant transformer saturation in the New Zealand electrical network.

Event 3b: We now contrast the GIC and THD response for Event 3b in Figure 6. For THD observations we therefore focus on the 10-min time period from 1:40-1:50 UT. The upper panels show the spatial variation in the high time resolution peak GIC values for all transformers where GIC are monitored, in the same format and axes ranges as Figure 5. A simple comparison between the upper right panels of Figure 5 and 6 shows that the peak GIC measured are 2-3 times smaller for Event 3b than the sudden commencement of Event 3a.

However, event 3b had long-lasting high GIC levels at Halfway Bush; the same time signature is seen in the majority of other substations with GIC monitoring. Because of that, more locations with clear GIC increases are seen in the lower left panel of Figure 6 when compared with the same panel of Figure 5. The largest average 10 min GIC magnitude is again seen in Dunedin at Halfway Bush (15.3 A), with the second highest in South Dunedin substation (11.3 A). The next largest average magnitude is seen in Invercargill (4.3 A), at the bottom of the South Island. For the 21 substations with active GIC monitors, the average GIC in this time period is 2.5 A, i.e. the 10 min average values for event 3b are a factor of 1.75 larger than for event 3a.

The lower right panel of Figure 6 provides an indication of the 10 min average $|H'|$ values from the magnetometers for event 3b. These span from ~10 nT/min (Swampy and

Middlemarch), Eyrewell (5.3 nT/min), and Te Wharau (3.7 nT/min). This period has more latitudinal variation than seen in event 3a.

The differences between the lower left panels of Figures 5 (event 3a) and 6 (event 3b) are clear, but not particularly dramatic. However, there is a much more significant difference between the even-THD maps in the lower right panels. Larger THD values, for event 3b compared with 3a, are seen throughout the South Island, as well as in the North Island, albeit at less significant levels. The largest even-THD percentage value is again seen at Black Point substation, but is now twice that seen earlier (0.4% c.f. 0.21%). Significant even-THD is seen in Dunedin, around Christchurch, and also on the West Coast of the South Island, stretching through the Tasman district. There is also a small but clear increase in multiple locations in Taranaki in the North Island. The mean even-THD across the country is slightly more than two and a half times larger than for event 3a. We now see that this condition was not unique to that substation but was widely true across the country. However, it is not true at all substations, likely due to the complex local variations in geoelectric field and the specific electrical network. Another factor is the differing nature of the transformers in different substations, which will saturate under differing conditions. For example, single-phase bank transformers are more susceptible than three-phase units [*NERC*, 2013]. The latter will produce much lower harmonics for a given DC neutral current input.

Event 4: Finally, we consider event 4. During this event there were GIC of >15 A occurring for ~30 minutes and peaking at ~49 A. The GIC and THD data is shown in Figure 7, in the same format as we used in Figures 5 and 6. This event has the highest peak GIC relative to events 3a and 3b for most, but not all transformers. The highest GIC magnitudes are seen in Dunedin, at the 2 DC monitored transformers in Halfway Bush (peaking at ~49 A and ~44 A) and at South Dunedin (39 A). Peak GIC magnitudes above 10 A are also seen for

transformers in Invercargill and Clyde. Previous studies have identified very high currents in Islington transformer number 6 [e.g., *Mac Manus et al.*, 2017; *Rodger et al.*, 2017; *Divett et al.*, 2018]. This is not seen for our analysis as the DC monitor for this transformer was not operational throughout the storm period.

As GIC magnitudes were significantly high for long time periods, we would expect the 10 min averaged GIC magnitude to be large. This is confirmed by the lower left panel of Figure 7, showing the average GIC magnitudes for each substation from 12:40-12:50 UT. For that time period the 10 min average GIC was measured as 21.5 A at Halfway Bush, 16.0 at South Dunedin, 6.6 A at Clyde, and 5.5 A at Invercargill. Noticeable GIC magnitudes are also present at multiple other locations, at least where DC monitors are deployed at one or more transformers in that substation. The mean GIC value is 4.1 A, a factor of 2.86 higher than event 3a (Figure 5) and 1.62 higher than the mean for event 3b (Figure 6). The high GIC magnitudes are associated with high average $|H'|$ values, as can be seen in the lower right panel of Figure 7. The largest average $|H'|$ values are seen in the lower South Island at Swampy (30.6 nT/min), with lower but still significant $|H'|$ values at Eyrewell (12.3 nT/min), and Te Wharau (7.9 nT/min).

The lower right panel of Figure 7 indicates that the even-THD distortion at 12:40-12:50 UT might be described as striking, particularly when compared with the quiet period (Figure 4) and event 3a (Figure 5). The mean even-THD percentage is 0.134%, 1.9 the level of Event 3b and 5 times that for Event 3a. The highest mean THD levels are seen in Dunedin substations (Halfway Bush with 0.73%, South Dunedin with 0.6%), but only slightly lower THD levels slightly south of Dunedin in Balclutha substation (0.54%), and at Black Point substation (0.5%). As one would expect, areas with significant GIC are associated with significant values of even-THD. However, there are also multiple large regions where large THD are

seen to occur where no GIC measurements are available. The occurrence of the large THD at those substations shows that there must have been significant GIC, in addition to the substations where GIC measurements were located. This is common from Christchurch northwards, but also in the West Coast/Tasman region in the northern part of the South Island, and in the northern parts of Taranaki in the North Island. In the latter case 5 of the 6 Taranaki substations show THD levels >0.2% in this time window, including: New Plymouth (0.28%), Carrington Street (0.27%), Motunui (0.25%), Huirangi (0.24%), and Stratford (0.21%). Only Hawera substation (0.14%), on the southern edge of the Taranaki region and seen by the smaller ring in Figure 7 (lower right panel), is below this somewhat arbitrary cutoff. There are also multiple examples of even-THD increases in the main North Island cities of Auckland and Wellington.

The levels of even-THD shown in the lower right panel of Figure 7 are the largest seen during the storming period. However, we note that this 10-min period is not the only time around Event 4 which includes significant even-THD seen widely across the New Zealand network. Noticeable even-THD is seen starting from the 10 minute period beginning at 12:10 UT, and lasting to the 10 min period which ends at 12:50 UT. For the period from 12:20-12:30 UT the levels are much like 12:40-12:50 UT (shown in Figure 7), while the 12:30-12:40 UT THD levels are slightly decreased. In contrast, the even harmonic distortion levels from 12:50 UT are very low, implying most transformer saturation issues have ended. We have provided a movie of the even-THD maps from 22:00 on 7 September 2017 to 15:00 on 8 September 2017, shown in the same format as the lower panels of Figure 7, which is available as supplementary material to the current study.

Overview Comments: It is worth contrasting the observed even-THD levels with international THD guidelines. For example the IEEE steady-state upper THD

613 recommendation is 1.5% for >161 kV [*IEEE Std 519–2014*, 2014], the International
614 Electrotechnical Commission (IEC) IEC 61000-3-6 recommendation is 3% [*McGranaghan*
615 *and Beaulieu*, 2006], or the New Zealand power quality guideline of 1.9% for high voltage
616 systems [*EEA*, 2013]. Clearly, none of the even-THD levels we report are hazardous.
617 However, we have demonstrated the presence of saturated transformers at multiple locations
618 across the South Island, as well as in Taranaki in the North Island. Despite this being a
619 comparatively small space weather disturbance, and not reaching the level of a major GMD,
620 both events 3b and 4 include widespread evidence of transformers operating with a degree of
621 half cycle saturation. The difference between the lower two panels of Figure 6 and 7 also
622 emphasizes the difference in the response one might conclude about the space weather risk
623 from the GIC measurements and the THD measurements. This is particularly noticeable
624 when the even-THD disturbances include multiple substations in the Taranaki region of the
625 North Island. Up to this point Transpower tended to view the space weather hazard as a lower
626 South Island issue, with little consideration of the North Island. The observations of clear
627 even-THD enhancements in Taranaki, implying saturated transformers during this
628 comparatively small GMD, has provoked much interest in Transpower; they have requested
629 modeling attention be extended to the North Island, and also are investigating installation of
630 new DC monitors for transformers in the North Island.
631
632 A feel for the harmonic amplitudes' decay with distance from their source transformers can
633 be found from the relative sizes of the half cycle saturation enhanced, percent-distortion
634 circles in maps like those in Figures 4-8 and in the supporting video. Of course, on some
635 occasions circles up to 100 km or so away from the largest circle are almost as large, likely
636 because the GIC-produced half cycle saturation is enhanced over the wide region. However,
637 for other active periods the sizes of the circles can be seen to decrease quite rapidly with
638 distance from an apparent source transformer, i.e., within several tens of km of the most

enhanced circle. This implies that, on these occasions, not only did the GIC-produced half cycle saturation not occur over a smaller spatial region but also that, generally, the observed harmonics decayed quite rapidly along the network power lines within distances of just several tens of km.

6. Implications for non-New Zealand locations

Section 5 implies that transformer saturation can occur for moderate GMD from the lowest part of New Zealand's South Island (the Tiwai substation located south of the city of Invercargill), equatorwards to at least the northern part of the Taranaki-region (near the city of New Plymouth). We assume that global locations within these geomagnetic latitude ranges might possibly have high enough GIC to produce transformer saturation and harmonic production, i.e., what occurs in New Zealand might happen elsewhere on Earth. We wish to consider how these locations correspond to other parts of the world, and use the International Geomagnetic Reference Field (IGRF), 12th Generation, revised in 2014 [*Thébault et al.*, 2015]. We use the online geomagnetic coordinate calculator provided by the British Geological Survey (http://www.geomag.bgs.ac.uk/data_service/models_compass/coord_calc.html).

Our most poleward THD-observing location was the Tiwai substation (46.59° S, 168.39° E). For epoch 2017.0 this geographical location has a quasi-dipole latitude of -53.92°, and a quasi-dipole longitude of 254.64°. This is geomagnetically equivalent to Aberdeen (Scotland; geographic: 57.15°N, 2.09°E, geomagnetic quasi-dipole: 53.93°, 81.54°) in Europe, and roughly equivalent to Vancouver (Canada; geographic: 49.28°N, 123.12°E, geomagnetic quasi-dipole: 54.19°, 299.22°) in North America and Magadan (Russia; geographic: 59.56°N, 150.83°E, geomagnetic quasi-dipole: 53.70°, 221.13°) in Eastern Asia. We note, however,

that the choice of the poleward limit for New Zealand is defined by the southern most edge of the New Zealand electrical transmission network. As such it is very likely that theoretical transformer locations further poleward of the Tiwai substation could well have experienced transformer saturation during this storm period in regions where networks extend to more poleward locations.

The equatorward-edge is therefore likely to be more interesting to the international community. We take the lower latitude edge to be represented by the substation in the city of New Plymouth (39.06°S, 174.08°E). For epoch 2017.0 this geographical location has a quasi-dipole latitude of -45.02°, and a quasi-dipole longitude of 257.16°. In contrast Luxembourg City (Luxembourg; geographic: 49.61°N, 6.13°E, geomagnetic quasi-dipole: 45.01°, 82.88°) in Europe is magnetically equivalent to New Plymouth, as is the North American city of Memphis (USA (Tennessee); geographic: 35.15° N, 90.05°W, geomagnetic quasi-dipole: 45.11°, 342.28°), or Charlotte (USA (North Carolina);geographic: 35.23° N, 80.84° W, geomagnetic quasi-dipole: 45.13°, 354.93°), or the East Asian city of Darkhan (Mongolia; geographic: 49.46° N, 105.97°W, geomagnetic quasi-dipole: 45.09°, 180.25°).

We caution, however, that the situation is clearly not as simple as simple geomagnetic latitude dependence, with the GIC magnitude depending strongly on the local ground conductivity structure (especially given the island nature of New Zealand, surrounded by deep conductive ocean),electrical network parameters and earthing setup, as well as the level of geomagnetic forcing. Only the geomagnetic forcing is likely to scale somewhat with geomagnetic latitude [e.g., *Shinbori et al.*, 2012]. Nonetheless we suggest the geomagnetic latitude of Taranaki is unusually equatorward to see evidence of GIC-produced transformer saturation for a storm which had maximum disturbance levels at ~12 UT on 8 September 2017 of Dst=-75 nT, AE=1335 nT, and Kp=8+, i.e., significantly disturbed, but hardly

extreme. It is also worth noting that GIC-linked transformer damage has been reported in South Africa at both Matimba Power Station (23.67°S, 27.44°E) and Lethabo Power Station (26.74°S, 27.98°E) [*Gaunt and Coetzee*, 2007]. These locations correspond to geomagnetic quasi-dipole coordinates of Matimba: -25.04°, 96.01° and Lethabo: -28.15°, 95.92°, which are ~20° equatorwards of New Plymouth.

7. September 2015: St Patrick's Day Storm THD

In the current study we have concentrated on the 7-8 September 2017 GMD interval, due to the existing literature indicating it is an interesting time interval to examine the variation of even-THD in New Zealand. As with any case-study interval, one might caution that we have considered only one storm, and questions arise as to the general applicability of the results. To test these concerns, we redid the THD analysis for the St. Patrick's Day 2015 GMD of 17 March 2015.

Some summary plots for this GMD are shown in Figure 8. The top left panel presents the EYR magnetometer $|H'|$ across the storm period, in both 1 min and 10 min resolution. The top right hand panel shows the magnitude of GIC measured at Halfway Bush transformer number 4. Based on this panel we have selected two time periods of interest, where the 10 min averaged GIC magnitude was significant: 09:50-10:00 UT, as well as the more significant 13:20-13:30 UT. We term these times St Pat's Event 1 and 2, respectively and mark them in the two upper panels of Figure 8. The lower two panels of the figure show the spatial variation in substorm average even-THD across New Zealand for these two time periods. While the patterns are not identical, there are similarities with the September 2017 events, with significant even-THD levels in the lower South Island, near Christchurch and the upper

South Island in West Coast/Tasman, and some level of even-THD enhancement in the North Island. In the later case while the Taranaki enhancements are not as pronounced, for St Pat's Event 1 even-THD enhancements are seen in two separate substations in the city of Hastings in the Hawke's Bay, located on the eastern edge of the North Island across from Taranaki; this location has a similar latitude to New Plymouth. We suggest this simple analysis confirms that there are differences in spatial response from storm to storm, but there are also wider similarities, indicative of consistent GIC "hot spots" (caused by the network configuration) and subsequent transformer saturation between different GMD events.

8. Summary and Discussion

There are multiple pathways by which GIC can adversely affect electrical power infrastructure through physical damage or disruption to supply during GMD. One of the pathways to disruption comes from the production of harmonic distortion to the AC waveform generated by half-cycle saturation of transformers. This is one of the few ways to produce even order harmonics (rather than odd harmonics).

Until now there has been limited simultaneous harmonic distortion experimental observations and GIC measurements presented in the literature. One reason for this may be that most countries have limited GIC measurements available to link to the harmonic distortion observations. However, New Zealand is unusually well positioned to investigate the occurrence of GIC in a mid-latitude country as there are comparatively large quantities of measurements available, including GIC in multiple locations and country-wide THD.

In this study we have examined even order harmonic distortion observations from the entire New Zealand network during the 7-8 September 2017 storm period. The analysis

shows that even-THD enhancements occur where there are significant GIC magnitudes which last over long time periods. However, these observations also demonstrate how GIC effects can be seen through even harmonic distortion in locations where no GIC measurements are present (for example, the upper South Island or the majority of the North Island). We have also examined a GMD from 17 March 2015, to test if there is some consistency between different geomagnetic storms. Our comparison suggests that while there is certainly variation in GIC and THD spatial variation from storm to storm, there are also gross similarities. Having identified substations on the northern part of Taranaki as a rough equatorward edge of the significant New Zealand-observed even-THD enhancements, we have noted this location corresponds to Luxembourg City in Europe or Memphis in North America.

We understand that harmonic distortion measurements are fairly common in electrical networks, much more so than DC measurements. DC measurements can also be inaccurate due to drift (corrected in our case through the removal of the HVDC stray currents following Mac Manus et al. [2017]). We suggest that further analysis of such datasets could allow a valuable new approach for the international Space Weather research community, if the commercial providers are willing to release those measurements.

Acknowledgments. This research was supported by the New Zealand Ministry of Business, Innovation & Employment Hazards and Infrastructure Research Fund Contract UOOX1502. The authors would like to thank Transpower New Zealand for supporting this study. Eyrewell magnetometer data availability is described at: http://www.intermagnet.org/imos/imos-list/imos-details-eng.php?iaga_code=EYR. Middlemarch and Te Wharau magnetometer data are available at the CRUX magnetometer array website (http://www1.osakac.ac.jp/crux/). The New Zealand LEM DC and harmonic

765 distortion data were provided to us by Transpower New Zealand with caveats and
766 restrictions. This includes requirements of permission before all publications and
767 presentations. In addition, we are unable to directly provide the New Zealand LEM DC data
768 or the derived GIC observations. Requests for access to the measurements need to be made
769 to Transpower New Zealand. At this time the contact point is Michael Dalzell
770 (Michael.Dalzell@transpower.co.nz). We are very grateful for the substantial data access
771 they have provided, noting this can be a challenge in the Space Weather field [*Hapgood and*
772 *Knipp,* 2016]. MAC would like to acknowledge support for this work from the Natural
773 Environment Research Council, NERC NE/P017231/1: Space Weather Impacts on Ground-
774 based Systems (SWIGS).
775

References

Arrillaga, J. and, N. R. Watson (2003), Power System Harmonics, 2nd Edition, Wiley, ISBN: 978-0-470-85129-6 October 2003.

Bailey, R. L., et al. (2017). Modelling geomagnetically induced currents in mid-latitude Central Europe using a thin-sheet approach. Annales Geophysicae, 5, 751–761. https://doi.org/10.5194/angeo-35-751-2017

Baker, D. N., et al. (2008), Severe Space Weather Events: Understanding Societal and Economic Impacts, 144 pp., National Academies Press, Washington, D. C., USA

Beggan, C. D., Beamish, D., Richards, A., Kelly, G. S., & Thomson, A. W. (2013). Prediction of extreme geomagnetically induced currents in the UK high-voltage network. Space Weather, 11, 407–419. https://doi.org/10.1002/swe.20065

Béland, J., and K. Small (2004), Space weather effects on power transmission systems: The cases of Hydro-Québec and Transpower New Zealand Ltd, in Effects of Space Weather on Technological Infrastructure, edited by I. A. Daglis, pp. 287–299, Kluwer Acad., Netherlands.

Blake, S. P., Gallagher, P. T., McCauley, J., Jones, A. G., Hogg, C., Campanyà, J., et al. (2016). Geomagnetically induced currents in the Irish power network during geomagnetic storms. Space Weather, 14, 1–19. https://doi.org/10.1002/2016SW001534

Bolduc, L. (2002), GIC observations and studies in the Hydro-Québec power system, Journal of Atmospheric and Solar-Terrestrial Physics, 64, 1793 – 1802.

Boteler, D. H. (2015). The Impact of Space Weather on the Electric Power Grid. In Heliophysics V. Space Weather and Society, by C. J. Schrijver, F. Bagenal, and Sojka. Palo Alto, CA: Lockheed Martin Solar & Astrophysics Laboratory

Boteler, D. H. (2019). A 21st century view of the March 1989 magnetic storm. Space Weather, 17, 1427– 1441. https://doi.org/10.1029/2019SW002278

Boteler, D.H., Shier, R.M., Watanabe, T. and Horita, R.E., Effects of geomagnetically induced currents in the BC Hydro 500 kV system, IEEE Trans. Power Delivery, 4, 818-823, 1989.

Boteler, D. H., & Pirjola, R. J. (2014). Comparison of methods for modelling geomagnetically induced currents. Annales Geophysicae, 32(9), 1177–1187. https://doi.org/10.5194/angeo-32-1177-2014

Chulliat, A., W. Brown, P. Alken, S. Macmillan, M. Nair, C. Beggan, A. Woods, B. Hamilton, B. Meyer and R. Redmon, 2019, Out-of-Cycle Update of the US/UK World

809 Magnetic Model for 2015-2020: Technical Note, National Centers for Environmental
810 Information, NOAA. doi: 10.25921/xhr3-0t19.
811 Clilverd, M. A., Rodger, C. J., Brundell, J. B., Dalzell, M., Martin, I., Mac Manus, D. H., et
812 al. (2018). Long-lasting geomagnetically induced currents and harmonic distortion
813 observed in New Zealand during the 7‐8 September 2017 disturbed period. Space
814 Weather, 16, 704– 717. https://doi.org/10.1029/2018SW001822
815 Crane, A. T. (1990). Physical vulnerability of electric systems to natural disaster and
816 sabotage, OTA-E-453 (p. 66). Washington, DC:U.S. Government Printing Office.
817 Dimmock, A. P., Rosenqvist, L., Hall, J.-O., Viljanen, A., Yordanova, E., Honkonen, I., et al.
818 (2019). The GIC and geomagnetic response over Fennoscandia to the 7‐8 September 2017
819 geomagnetic storm. Space Weather, 17, 989-1010.
820 https://doi.org/10.1029/2018SW002132.
821 Divett, T., G. S. Richardson, C. D. Beggan, C. J. Rodger, D. H. Boteler, and M. Ingham
822 (2018), Transformer-level modeling of Geomagnetically Induced Currents in New
823 Zealand's South Island, Space Weather, 16, 718–735, doi:
824 http://dx.doi.org/10.1029/2018SW001814.
825 Divett, T., M. Ingham, C. D. Beggan, G. S. Richardson, C. J. Rodger, A. W. P. Thom- son,
826 and M. Dalzell (2017), Modeling Geoelectric Fields and Geomagnetically Induced
827 Currents Around New Zealand to Explore GIC in the South Island's Electrical Trans-
828 mission Network, Space Weather, 15(10), 1396–1412, doi:10.1002/2017SW001697.
829 Eastwood, J. P., Biffis, E. , Hapgood, M. A., Green, L. , Bisi, M. M., Bentley, R. D., Wicks,
830 R. , McKinnell, L. , Gibbs, M. and Burnett, C. (2017), The Economic Impact of Space
831 Weather: Where Do We Stand?. Risk Analysis, 37: 206-218. doi:10.1111/risa.12765
832 EEA (2013), Power Quality Guide (Update and Amendment) 2013, Electricity Engineers'
833 Association of NZ (EEA). Available online from:
834 https://www.eea.co.nz/tools/products/details.aspx?SECT=publications&ITEM=2577.
835 EPRI (1983), Mitigation of geomagnetically induced and dc stray currents, EPRI, Palo Alto,
836 CA: Report EL-3295.
837 EPRI (2014), Analysis of Geomagnetic Disturbance (GMD) Related Harmonics, EPRI, Palo
838 Alto, CA: 2014. 3002002985.
839 Gaunt, C.T. & Coetzee, G. (2007), Transformer failures in regions incorrectly considered to
840 have low GIC risk, Power Tech, 2007 IEEE Lausanne, 807 -812,
841 10.1109/PCT.2007.4538419.

Gorman, P. (2012). Transpower battens down for Sun storms, The Press. Available online from: http://www.stuff.co.nz/the-press/news/6664044/Transpower-battens-down-for-sun-storms (accessed 2 August 2019).

Guillon, S., P. Toner, L. Gibson, and D. Boteler (2016), A Colorful Blackout, IEEE Power & Energy Mag., doi:10.1109/MPE.2016.2591760.

Hapgood, M., and D. J. Knipp (2016), Data Citation and Availability: Striking a Balance Between the Ideal and the Practical, Space Weather, 14, 919–920, doi:10.1002/2016SW001553.

IEEE Std 519-2014 (2014). IEEE recommended practice and requirements for harmonic control in electric power systems. IEEE Std 519–2014 (Revision of IEEE Std 519–1992) pp. 1–29.

Ingham, M., C. J. Rodger, T. Divett, M. Dalzell, and T. Petersen, Assessment of GIC based on transfer function analysis, Space Weather, 15, doi:10.1002/2017SW001707, 5, 1615–1627, 2017.

JASON (2011), Impacts of Severe Space Weather on the Electric Grid (JSR-11-320), The MITRE Corporation, McLean, Virginia, USA.

Knipp, D. J., et al. (2016), The May 1967 great storm and radio disruption event: Extreme space weather and extraordinary responses, Space Weather, 14, 614–633, doi:10.1002/2016SW001423.

Knipp, D. J., Fraser, B. J., Shea, M. A., & Smart, D. F. (2018). On the little‐known consequences of the 4 August 1972 ultra - fast coronal mass ejecta: Facts, commentary, and call to action. Space Weather, 16, 1635-1643. https://doi.org/10.1029/2018SW002024

Love, J. J., and P. Coïsson (2016), The geomagnetic blitz of September 1941, Eos, 97, doi:10.1029/2016EO059319. Published on 15 September 2016.

McGranaghan, M., and G. Beaulieu (2006). Update on IEC 61000-3-6: Harmonic Emission Limits for Customers Connected to MV, HV, and EHV. 2005/2006 IEEE/PES Transmission and Distribution Conference and Exhibition Proceedings, DOI: 10.1109/TDC.2006.1668668.

Mac Manus, D. H., Rodger, C. J., Dalzell, M., Thomson, A. W. P., Clilverd, M. A., Petersen, T. et al. (2017). Long term Geomagnetically Induced Current Observations in New Zealand: Earth return Corrections and Geomagnetic Field Driver. Space Weather, 15, 1020–1038, doi:10.1029/2017SW001635.

874 Marshall, R. A., M. Dalzell, C. L. Waters, P. Goldthorpe, and E. A. Smith (2012),
875 Geomagnetically induced currents in the New Zealand power network, Space Weather, 10,
876 S08003, doi:10.1029/2012SW000806.
877 North American Electric Reliability Corporation (NERC). 2012 Special Reliability
878 Assessment Interim Report: Effects of Geomagnetic Disturbances on the Bulk Power
879 System. 2012. Available online:
880 https://www.eenews.net/assets/2012/02/29/document_pm_01.pdf (accessed on 1 August
881 2019).
882 North American Electric Reliability Corporation (NERC). Network Applicability Project
883 2013-03 (Geomagnetic Disturbance Mitigation) EOP-010-1 (Geomagnetic Disturbance
884 Operations). 2013. Available online:
885 https://www.nerc.com/pa/Stand/Project201303GeomagneticDisturbanceMitigation/Applic
886 ableNetwork_clean.pdf (accessed on 1 October 2019).
887 Obana, Y., Waters, C. L., Sciffer, M. D., Menk, F. W., Lysak, R. L., Shiokawa, K. et al.
888 (2015). Resonance structure and mode transition of quarter-wave ULF pulsations around
889 the dawn terminator. J. Geophys. Res. Space Physics, 120, 4194–4212. doi:
890 10.1002/2015JA021096.
891 Oughton, E. J., A. Skelton, R. B. Horne, A. W. P. Thomson, and C. T. Gaunt (2017),
892 Quantifying the daily economic impact of extreme space weather due to failure in
893 electricity transmission infrastructure, Space Weather, 15, doi:10.1002/2016SW001491.
894 Rodger, C. J., et al. (2017). Long-term geomagnetically induced current observations from
895 New Zealand: Peak current estimates for extreme geomagnetic storms. Space Weather, 15,
896 1447–1460. https://doi.org/10.1002/2017SW001691.
897 Samuelsson, O. (2013). Geomagnetic Disturbances and Their Impact on Power Systems -
898 Status Report 2013. Sweden: Lund University.
899 Shinbori, A., Tsuji, Y., Kikuchi, T., Araki, T., Ikeda, A., Uozumi, T., Baishev, D., Shevtsov,
900 B. M., Nagatsuma, T., and Yumoto, K. (2012), Magnetic local time and latitude
901 dependence of amplitude of the main impulse (MI) of geomagnetic sudden
902 commencements and its seasonal variation, J. Geophys. Res., 117, A08322,
903 doi:10.1029/2012JA018006.
904 Thébault, E., C. C. Finlay, C. D. Beggan, P. Alken, J. Aubert, O. Barrois, F. Bertrand, T.
905 Bondar, A. Boness, L. Brocco, E. Canet, A. Chambodut, A. Chulliat, P. Coïsson, F. Civet,
906 A. Du, A. Fournier, I. Fratter, N. Gillet, B. Hamilton, M. Hamoudi, G. Hulot, T. Jager, M.
907 Korte, W. Kuang, X. Lalanne, B. Langlais, J.-M. Léger, V. Lesur, F. J. Lowes, S.

908 Macmillan, M. Mandea, C. Manoj, S. Maus, N. Olsen, V. Petrov, V. Ridley, M. Rother,
909 T. J. Sabaka, D. Saturnino, R. Schachtschneider, O. Sirol, A. Tangborn, A. Thomson, L.
910 Tøffner-Clausen, P. Vigneron, I. Wardinski, and T. Zvereva, International Geomagnetic
911 Reference Field: the 12th generation, Earth, Planets and Space., 67 (1).
912 doi:10.1186/s40623-015-0228-9, 2015.
913 Transpower (2015). Manage geomagnetic induced currents, Rep. PR-DP-252/V05-03, Syst.
914 Oper. Div., Wellington.
915 Transpower (2019). Map of New Zealand showing substations and transmission lines updated
916 May 2019. Available online from https://www.transpower.co.nz/system-operator/key-
917 documents/maps-and-diagrams (downloaded 2 August 2019).
918 United Nations Committee on the Peaceful Uses of Outer Space Expert Group on Space
919 Weather (2017), Report on Thematic Priority 4: International Framework for Space
920 Weather Services for UNISPACE+50 (A/AC.105/1171). Available online from:
921 www.unoosa.org/oosa/oosadoc/data/documents/2018/aac.105/aac.1051171_0.html
922 Walling, R.A., and A.H. Khan, Characteristics of Transformer Exciting Current During
923 Geomagnetic Disturbances, IEEE Trans. Power Delivery, Vol. 6, No. 4, October 1991.
924
925 ___

926 James B. Brundell, Tim Divett, Daniel H. Mac Manus, Craig J. Rodger, and Neil. R.
927 Thomson, Department of Physics, University of Otago, P.O. Box 56, Dunedin, New Zealand.
928 (email: james@brundell.co.nz, tdivett@gmail.com, macda381@student.otago.ac.nz,
929 crodger@physics.otago.ac.nz, n_thomson@physics.otago.ac.nz).
930 Mark A. Clilverd, British Antarctic Survey (UKRI-NERC), High Cross, Madingley Road,
931 Cambridge CB3 0ET, England, U.K. (e-mail: macl@bas.ac.uk).
932 Michael Dalzell and Ian Martin, Transpower New Zealand Ltd, Waikoukou, 22 Boulcott
933 Street, PO Box 1021, Wellington, New Zealand. (email: Michael.Dalzell@transpower.co.nz;
934 Ian.Martin@ems.co.nz).
935 Yuki Obana, Osaka Electro-Communication University, Neyagawa, Osaka, Japan. (email:
936 obana@osakac.ac.jp).

Tanja Petersen, GNS Science, 1 Fairway Drive, Avalon, Lower Hutt 5011, New Zealand (email: T.Petersen@gns.cri.nz).

Neville Watson, College of Engineering, University of Canterbury, 69 Creyke Road Christchurch, New Zealand (email: neville.watson@canterbury.ac.nz).

945

Date	Total Transformers Monitored	Total Substations Monitored
Nov 2001	36	13
Mar 2002	37	13
Sep 2002	38	13
Jan 2005	39	13
Apr 2005	41	13
Sep 2008	42	13
Feb 2009	43	14
Mar 2009	45	14
Apr 2009	46	14
Jul 2010	47	14
Sep 2010	46	14
Aug 2011	45	14
Nov 2011	47	15
Dec 2011	48	15
Oct 2012	53	18
Nov 2012	52	18
Dec 2012	54	19
Feb 2013	63	21
Mar 2013	62	21
May 2013	63	21
Aug 2013	64	21
Jan 2014	65	21
Jun 2015	66	21
Jan 2017	65	21
Feb 2017	64	21
Apr 2017	63	21
Jun 2017	62	21
Oct 2017	60	21
Dec 2017	58	20
Jan 2018	59	20
Feb 2018	58	20
Jun 2018	60	21
Nov 2018	60	22

946

947 **Table 1.** Change with time in the number of South Island transformers and substations for
948 which DC monitoring systems were operating at locations shown in Figure 1. Note that this
949 is an update to Table 1 from *Mac Manus et al.* [2017], reflecting new information from
950 Transpower New Zealand Ltd.

951

952

953

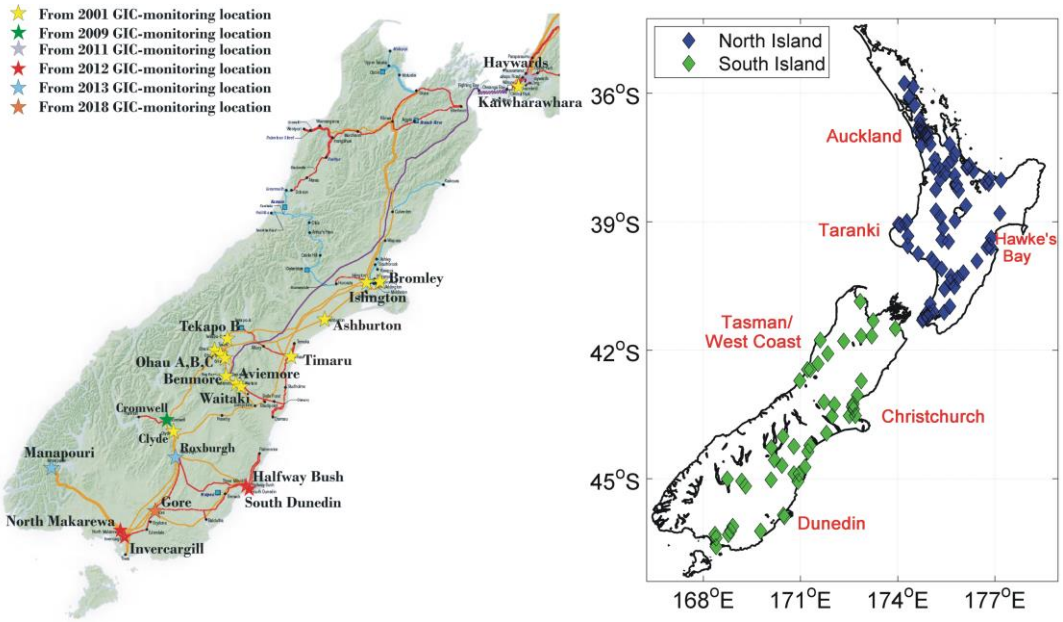

Figure 1. Left hand panel: Map of the South Island of New Zealand showing the Transpower New Zealand electrical transmission network, updating Figure 1 from *Mac Manus et al.* [2017], reflecting new information from Transpower New Zealand Ltd. Stars show the location of substations containing the LEM DC monitoring equipment, the data from which can be corrected to produce GIC measurements. Substations without DC monitoring equipment are shown by the small blue squares. Right hand panel: Locations of the even-THD observations used in the current study. A total of 126 substations provide even-THD measurements, covering the entire Transpower electricity transmission network.

968

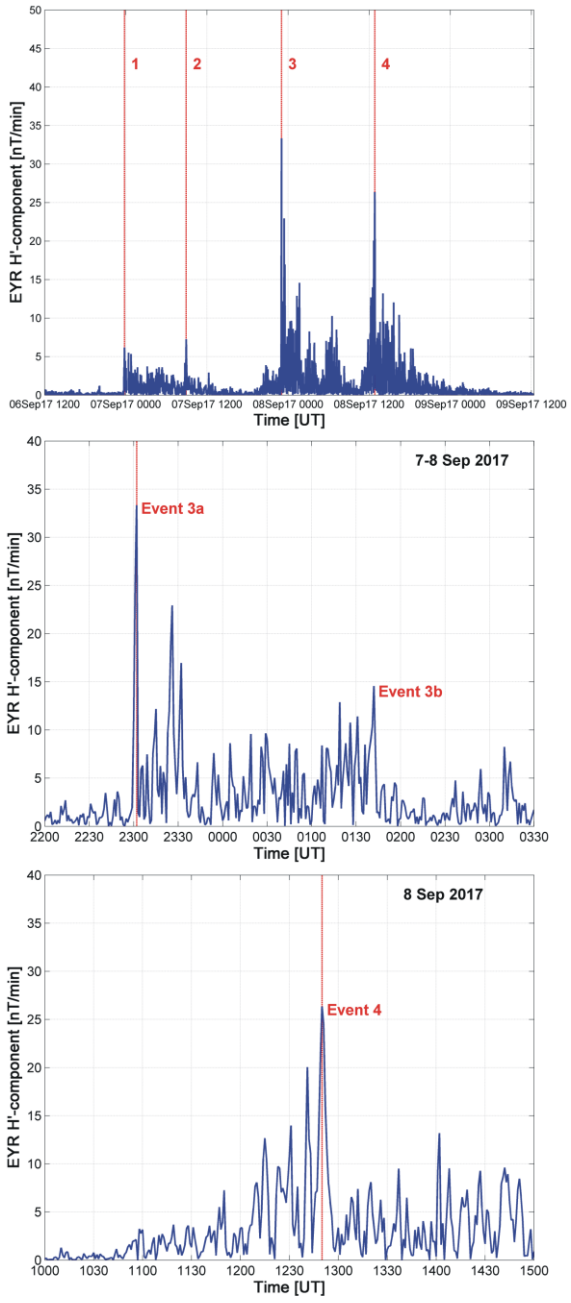

969
970

971 **Figure 2.** Upper panel: Magnitude of the rate of change of the horizontal component (|*H'*|)
972 of the magnetic field observed by the EYR magnetometer during the 6-9 September 2017
973 series of GMD. Four time periods are marked by red lines, based on the times of four
974 distinct peaks in the magnitude of the rate of change of the *H*-component of the EYR data,
975 as discussed in the text. Middle panel: Detailed examination of the EYR |*H'*| for the time
976 period around Event 3. Lower panel: As the middle panel, but for the Event 4 time period.

977

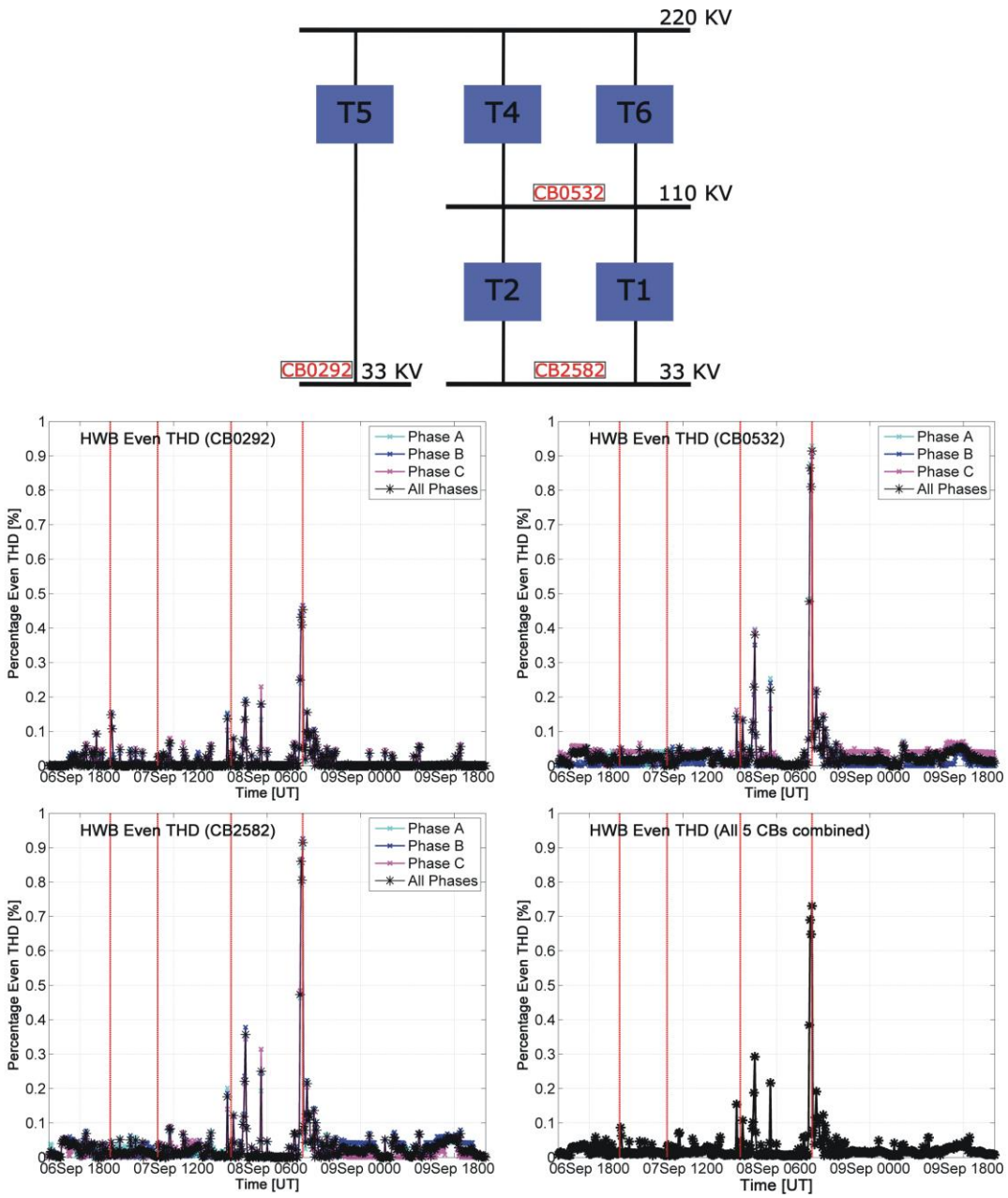

Figure 3. Upper panel: A single line diagram of the Halfway Bush (HWB) substation electrical connections. The red boxes mark HWB T4, and the locations of the 5 circuit breakers (CB) which have even total harmonic distortion (THD) measurements. See text for more details. Lower panels: Even-THD observations at each CB, as labelled, recording separately the 3 phases and the mean of all phases. The lower right hand panel shows the combined mean of all 15 observations, representing the time-varying summary even-THD for the HWB substation.

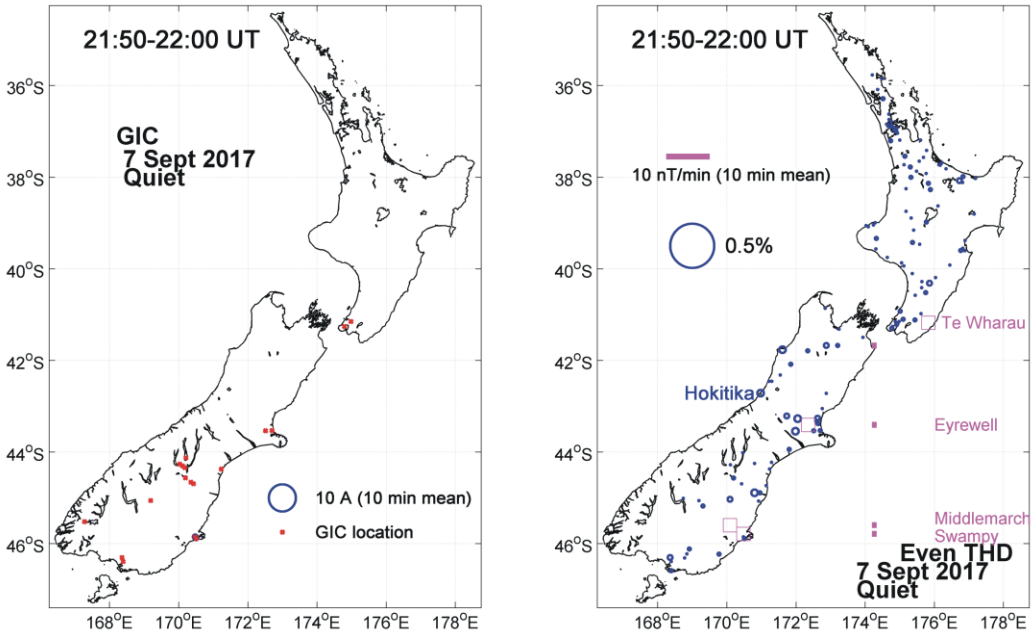

Figure 4. A comparison of the GIC and THD observations for 21:50-22:00 UT on 7 September 2017. This time is selected as a fairly quiet reference as it is only weakly disturbed. Left panel: Indications of the 10 min average GIC magnitude at the locations where these observations exist (red crosses). Right panel: Indication of the even-THD disturbance levels at the same time. The magnetometer sites are marked by magenta boxes, with bars at 174.2ºE showing the value of $|H'|$ at each of these sites.

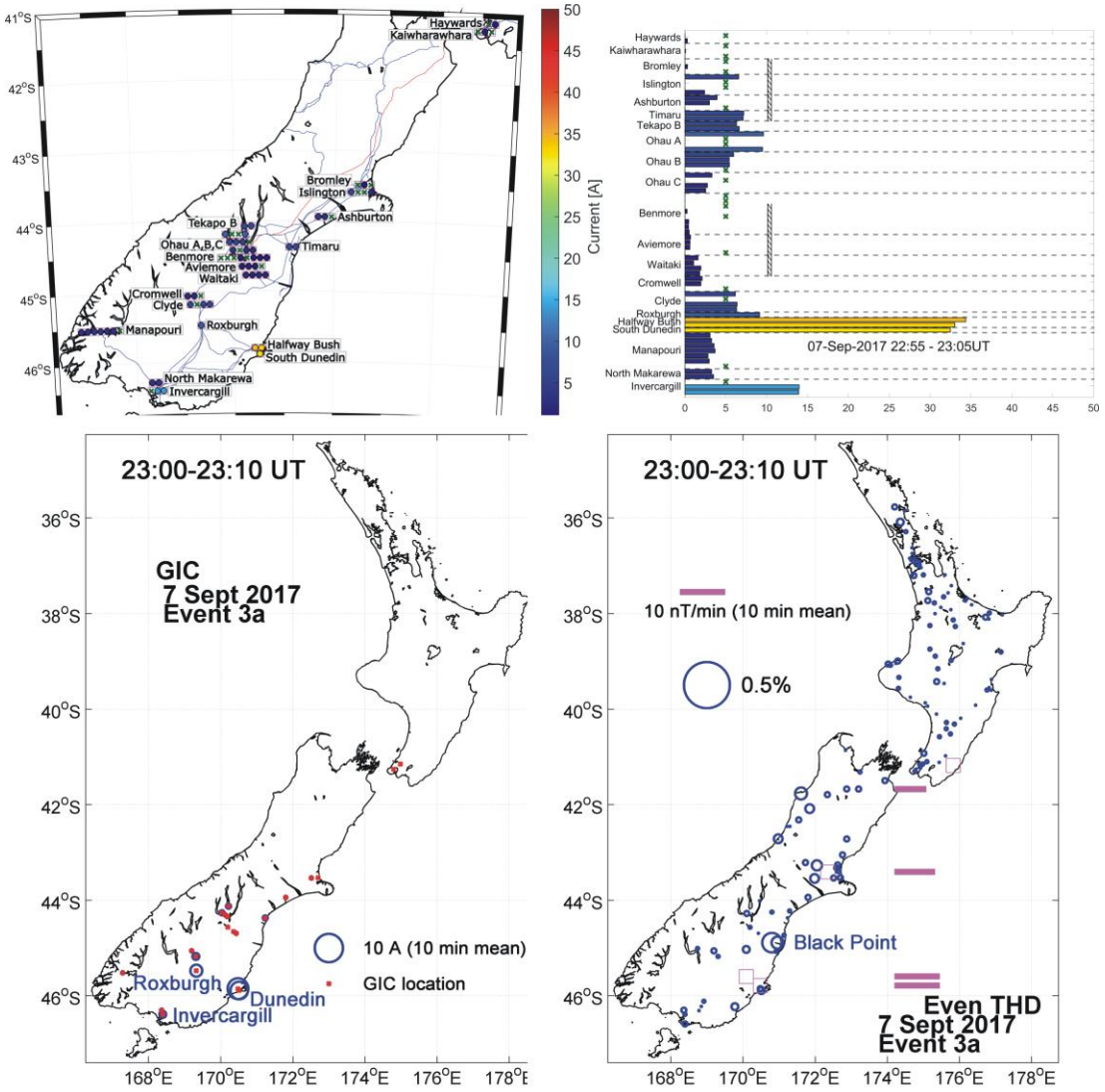

Figure 5. Observations during Event 3a, the arrival of the second sudden commencement solar wind shock arrival. The upper two panels show how the peak 4 s resolution GIC magnitudes vary between transformers during the shock arrival. The lower two panels are a comparison of the 10 min resolution GIC and THD observations, in the same format as Figure 4.

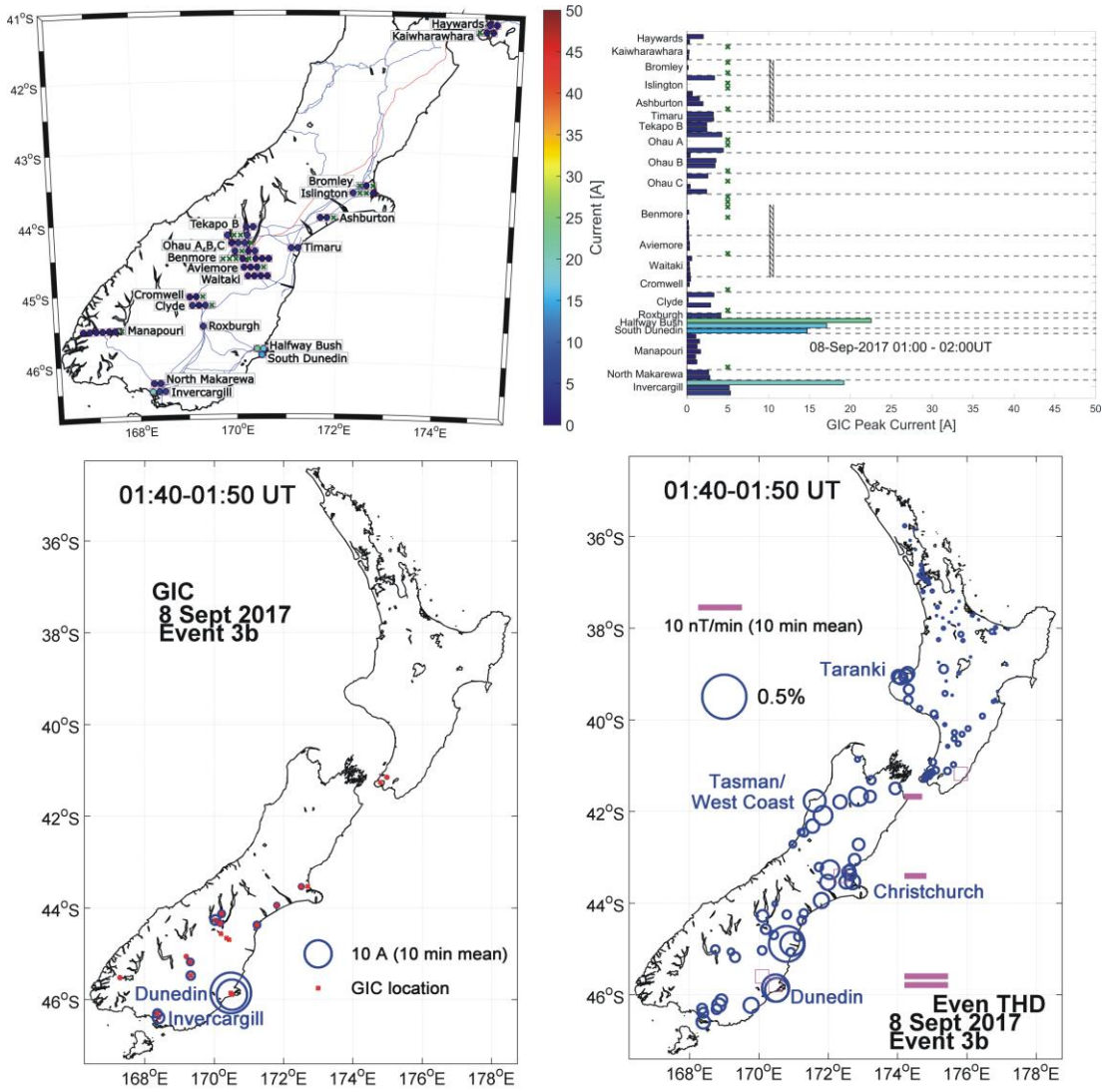

Figure 6. Observations during Event 3b, two and a half hours after the second sudden commencement solar wind shock arrival. All four panels are in the same format as Figure 5, but for the differing time period, as labeled.

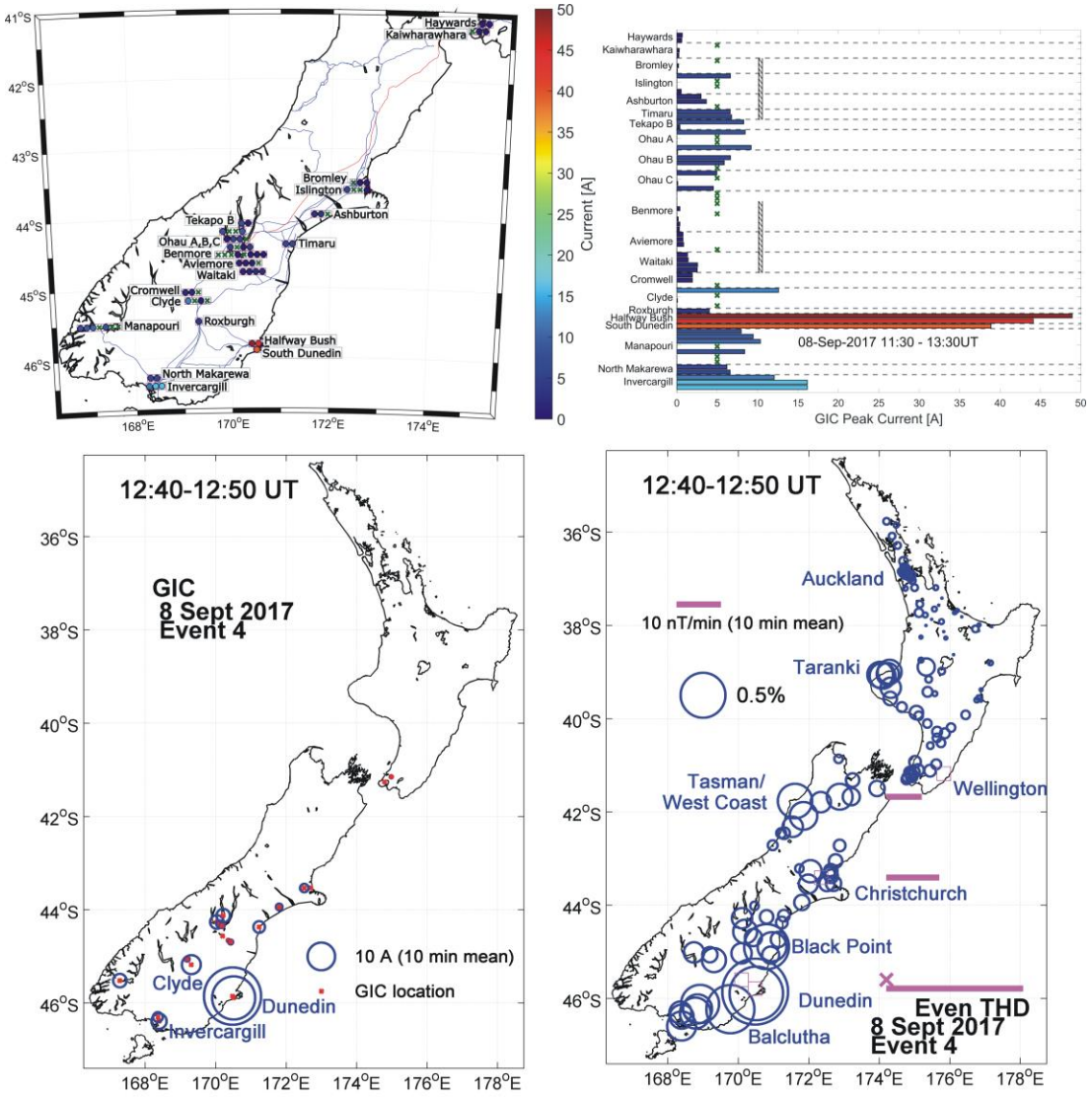

Figure 7. Observations during Event 4, thirteen and a half hours after the second sudden commencement solar wind shock arrival. All four panels are in the same format as Figure 5, but for the differing time period, as labeled. Note the presence of clear THD increases in the North Island.

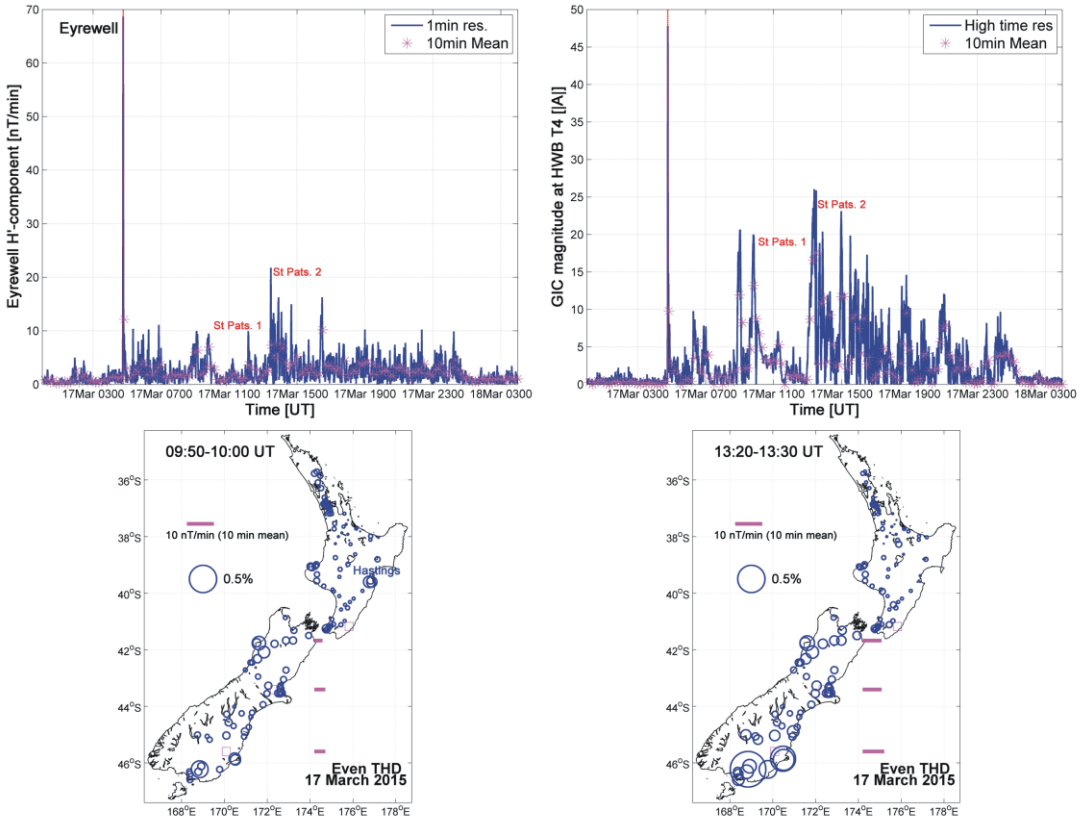

Figure 8. GIC and even-THD observations during the St Patrick's Day 2015 GMD (17 March 2015). In order the panels show: (upper left) Magnitude of the EYR horizontal component rate of change of the ($|H'|$); (upper right) GIC magnitude measured at Halfway Bush (HWB) transformer number 4; (lower left) map of even-THD increases in the same format as seen in Figures 4-7, but now for 9:50-10:00 UT on 17 March 2015; (lower right), as the previous panel but for 13:20-13:30 UT.

Figure 1.

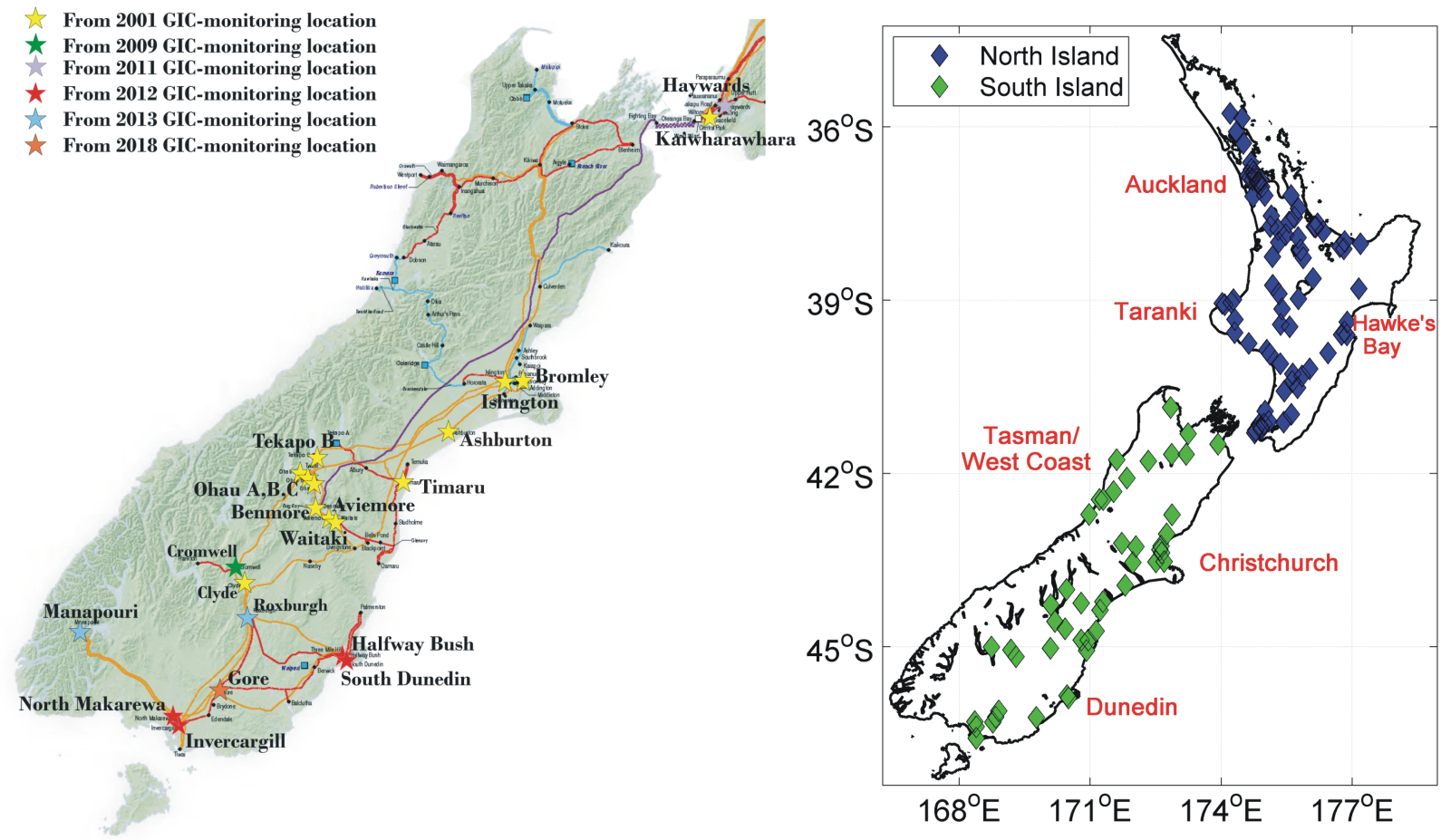
From 2001 GIC-monitoring location
From 2009 GIC-monitoring location
From 2011 GIC-monitoring location
From 2012 GIC-monitoring location
From 2013 GIC-monitoring location
From 2018 GIC-monitoring location
Haywards
Kaiwharawhara
Bromley
Islington
Ashburton
Tekapo B
Ohau A,B,C
Timaru
Aviemore
Benmore
Waitaki
Cromwell
Clyde
Roxburgh
Manapouri
Halfway Bush
South Dunedin
Gore
North Makarewa
Invercargill
North Island
South Island
36°S
39°S
42°S
45°S
168°E
171°E
174°E
177°E
Auckland
Taranki
Hawke's Bay
Tasman/ West Coast
Christchurch
Dunedin

Figure 2.

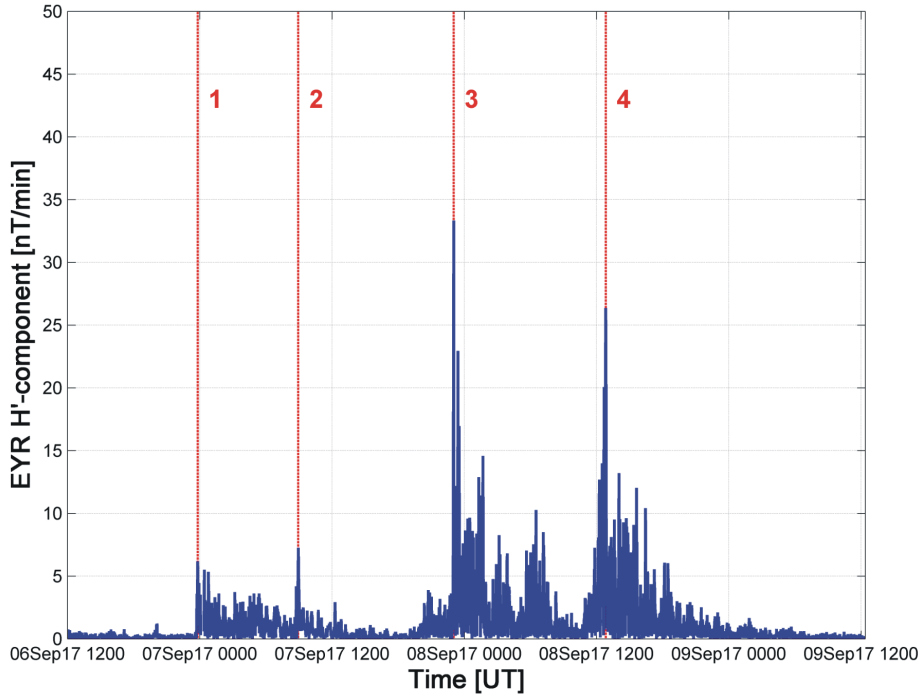
1
2
3
4
EYR H'-component [nT/min]
0
5
10
15
20
25
30
35
40
45
50
06Sep17 1200
07Sep17 0000
07Sep17 1200
08Sep17 0000
08Sep17 1200
09Sep17 0000
09Sep17 1200
Time [UT]

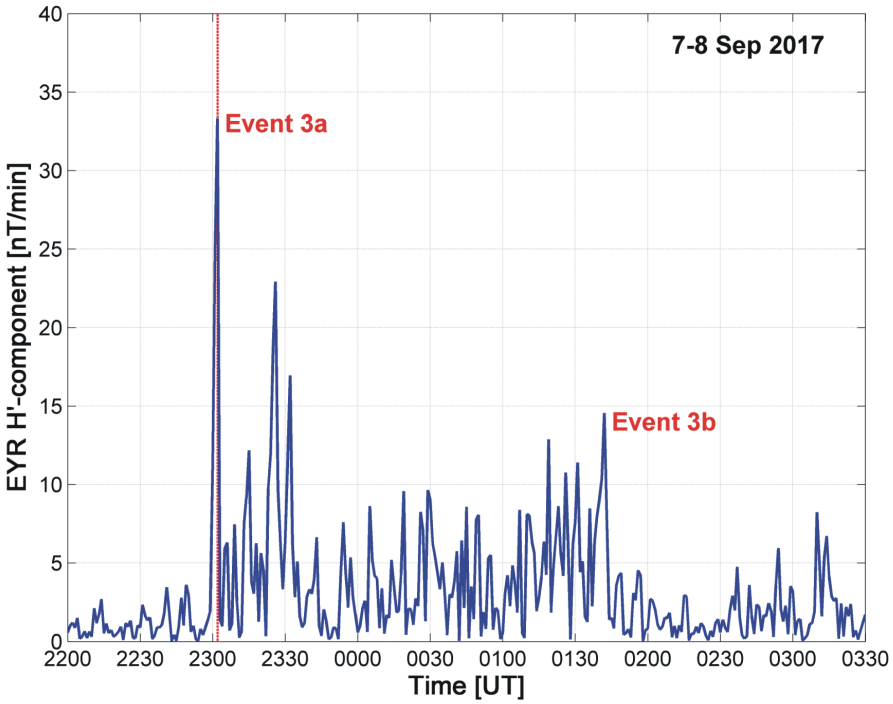
7-8 Sep 2017
Event 3a
Event 3b
EYR H'-component [nT/min]
0
5
10
15
20
25
30
35
40
2200
2230
2300
2330
0000
0030
0100
0130
0200
0230
0300
0330
Time [UT]

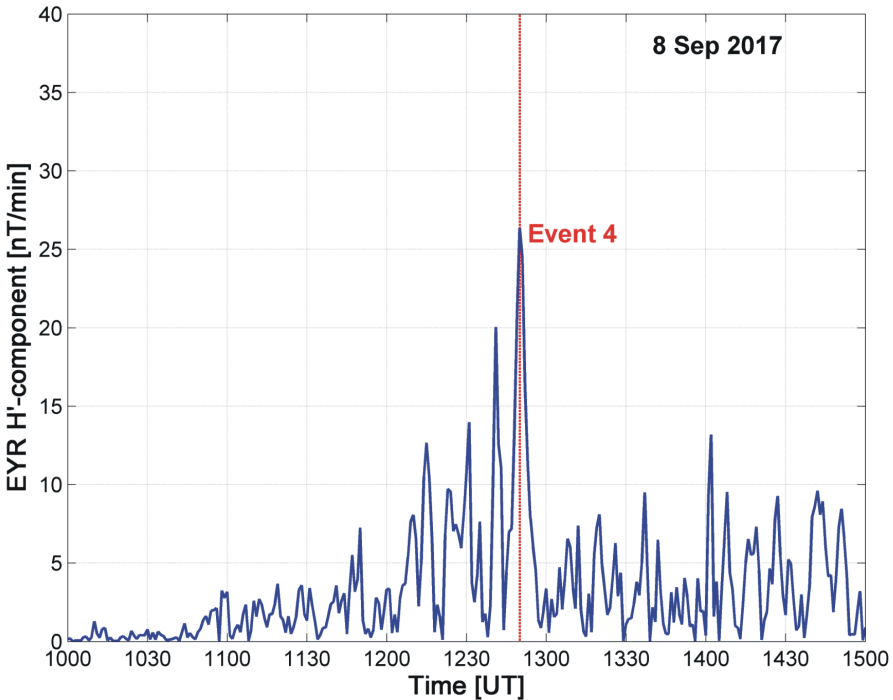
8 Sep 2017
Event 4
EYR H'-component [nT/min]
0
5
10
15
20
25
30
35
40
1000
1030
1100
1130
1200
1230
1300
1330
1400
1430
1500
Time [UT]

Figure 3.

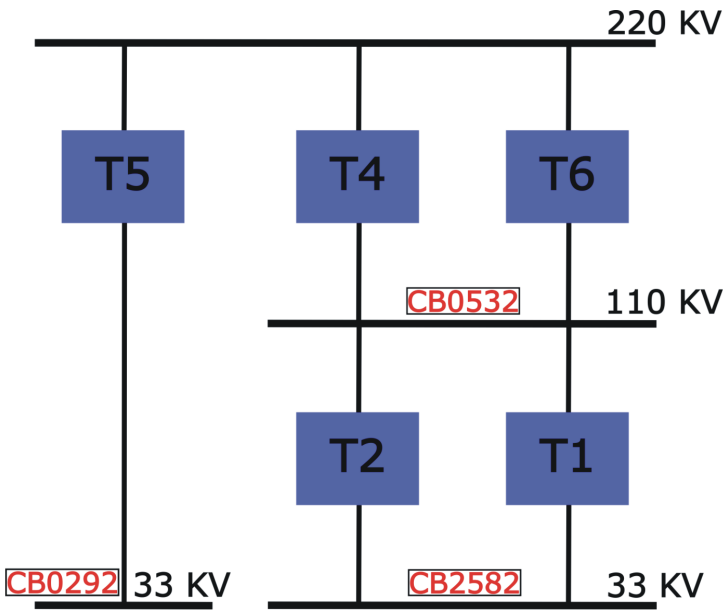
220 KV
T5
T4
T6
CB0532
110 KV
T2
T1
CB0292
33 KV
CB2582
33 KV

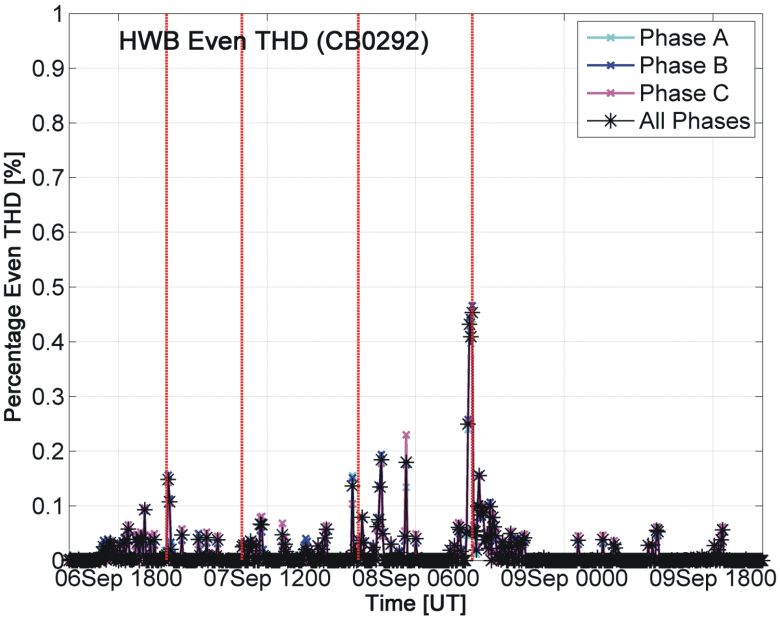
HWB Even THD (CB0292)
Phase A
Phase B
Phase C
All Phases
Percentage Even THD [%]
Time [UT]
06Sep 1800
07Sep 1200
08Sep 0600
09Sep 0000
09Sep 1800

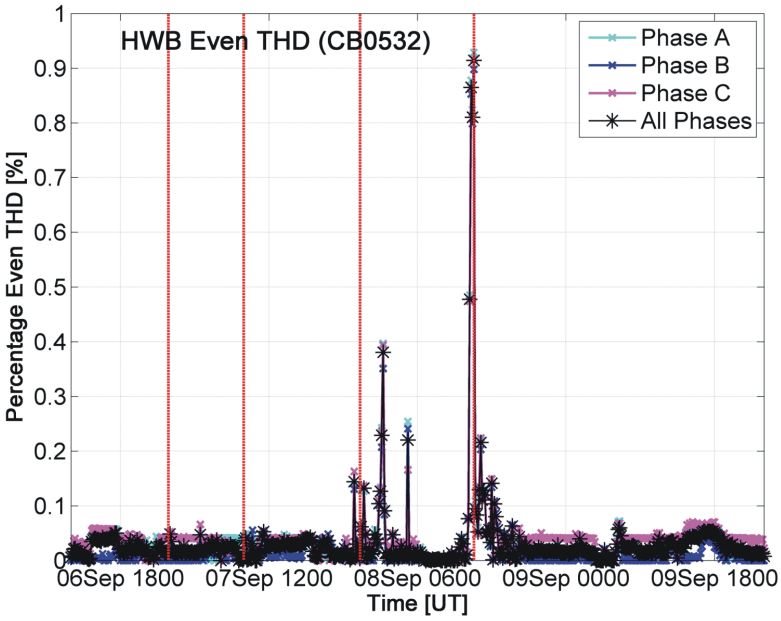
HWB Even THD (CB0532)
Phase A
Phase B
Phase C
All Phases
Percentage Even THD [%]
Time [UT]
06Sep 1800
07Sep 1200
08Sep 0600
09Sep 0000
09Sep 1800

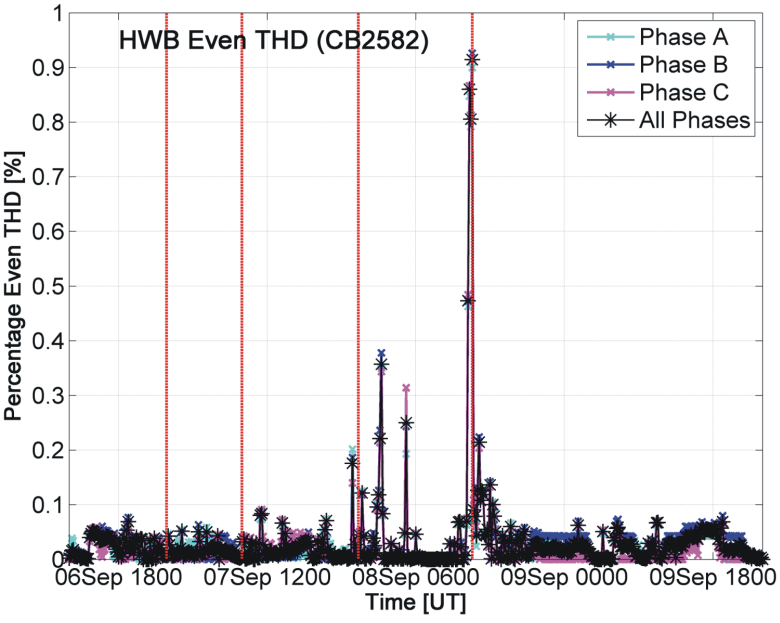
HWB Even THD (CB2582)
Phase A
Phase B
Phase C
All Phases
Percentage Even THD [%]
Time [UT]
06Sep 1800
07Sep 1200
08Sep 0600
09Sep 0000
09Sep 1800

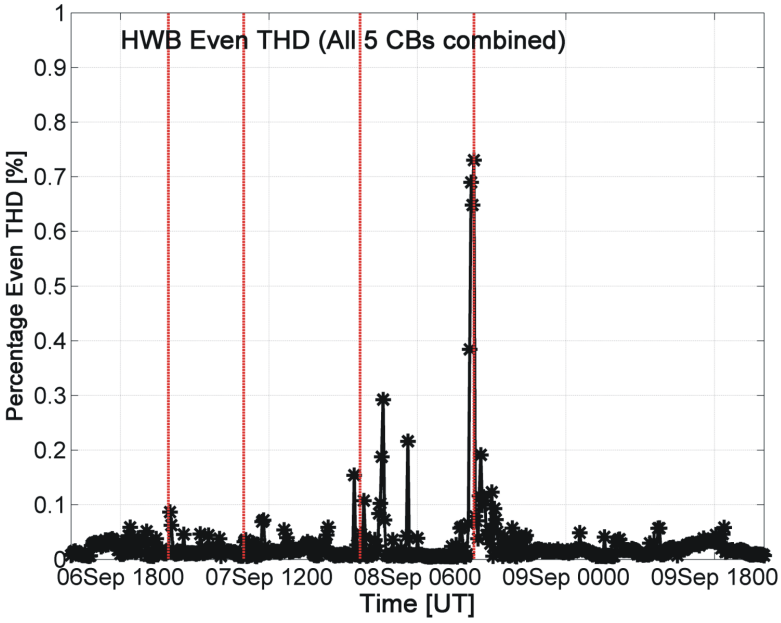
HWB Even THD (All 5 CBs combined)
Percentage Even THD [%]
Time [UT]
06Sep 1800
07Sep 1200
08Sep 0600
09Sep 0000
09Sep 1800

Figure 4.

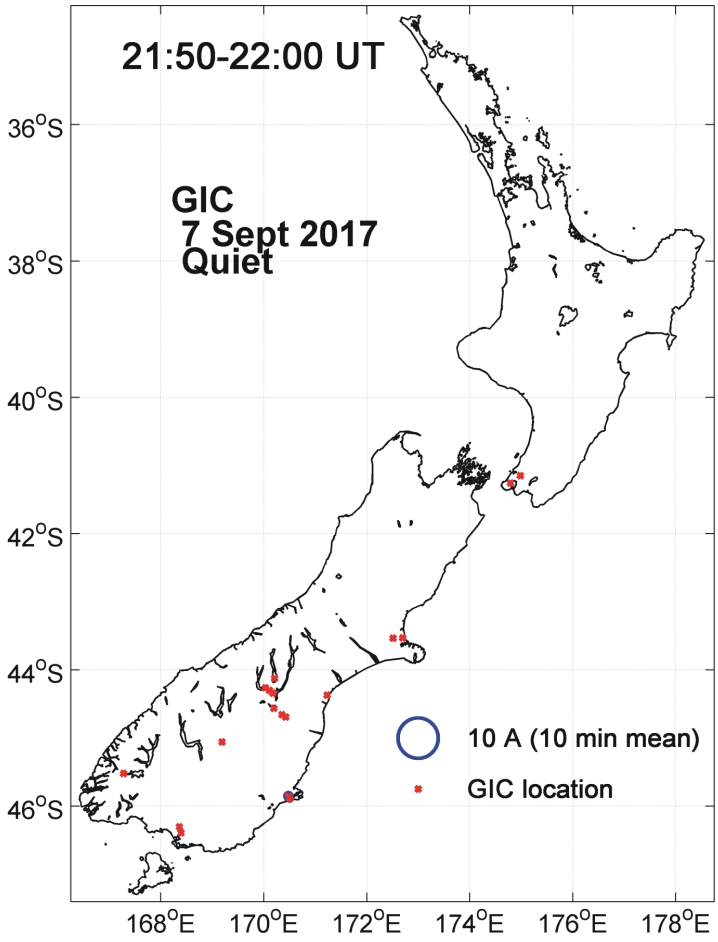
21:50-22:00 UT
GIC
7 Sept 2017
Quiet
10 A (10 min mean)
GIC location
36°S
38°S
40°S
42°S
44°S
46°S
168°E
170°E
172°E
174°E
176°E
178°E

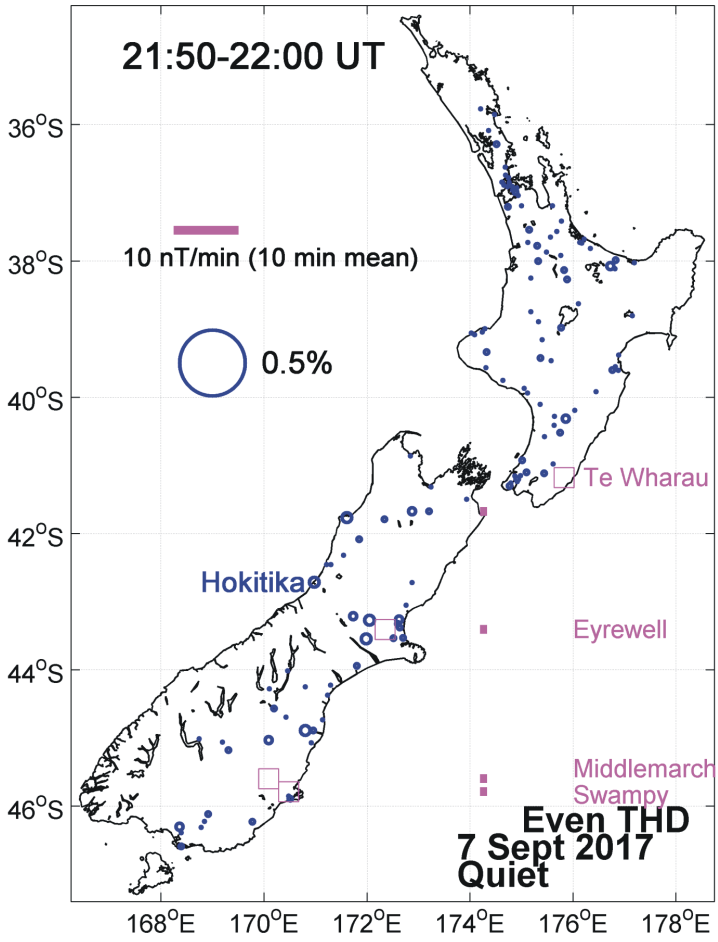
21:50-22:00 UT
10 nT/min (10 min mean)
0.5%
Te Wharau
Hokitika
Eyrewell
Middlemarch
Swampy
Even THD
7 Sept 2017
Quiet
36°S
38°S
40°S
42°S
44°S
46°S
168°E
170°E
172°E
174°E
176°E
178°E

Figure 5.

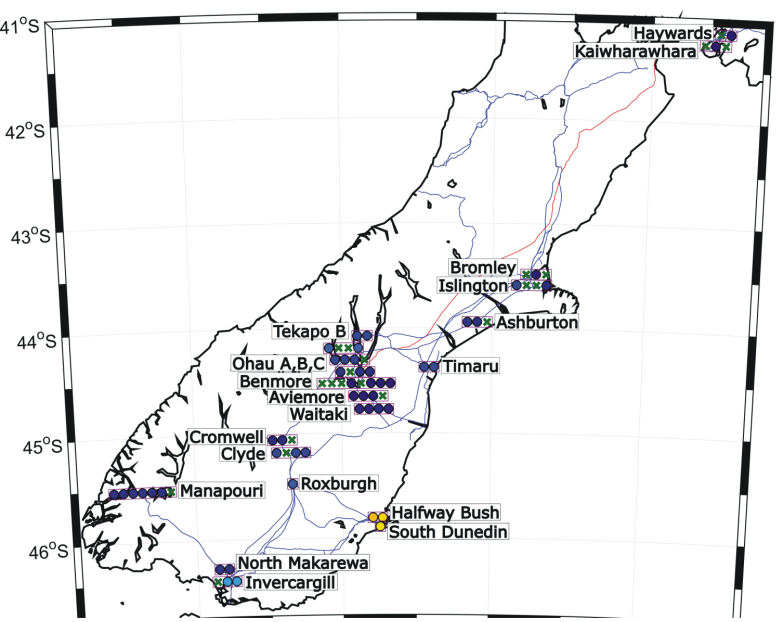
41°S
42°S
43°S
44°S
45°S
46°S
Haywards
Kaiwharawhara
Bromley
Islington
Ashburton
Tekapo B
Ohau A,B,C
Timaru
Benmore
Aviemore
Waitaki
Cromwell
Clyde
Roxburgh
Manapouri
Halfway Bush
South Dunedin
North Makarewa
Invercargill

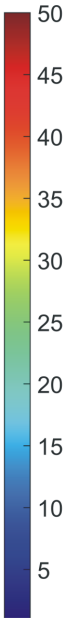
50
45
40
35
30
25
20
15
10
5
Current [A]

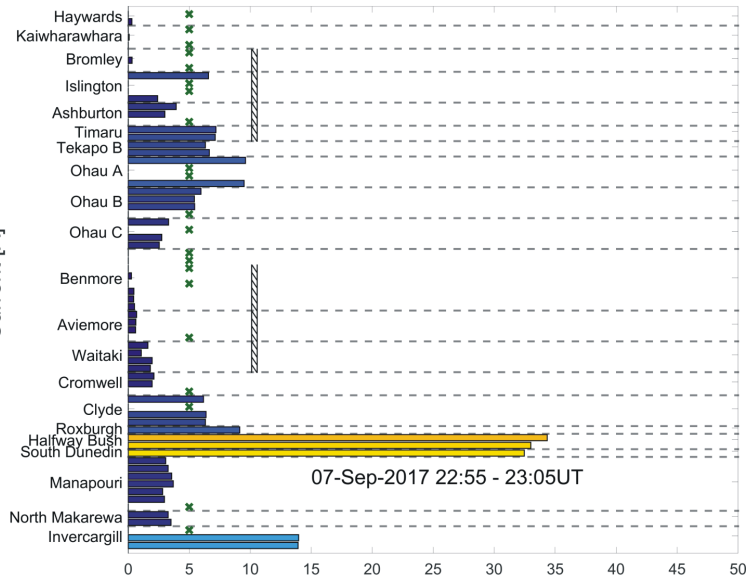
Haywards
Kaiwharawhara
Bromley
Islington
Ashburton
Timaru
Tekapo B
Ohau A
Ohau B
Ohau C
Benmore
Aviemore
Waitaki
Cromwell
Clyde
Roxburgh
Halfway Bush
South Dunedin
Manapouri
North Makarewa
Invercargill
07-Sep-2017 22:55 - 23:05UT
0
5
10
15
20
25
30
35
40
45
50

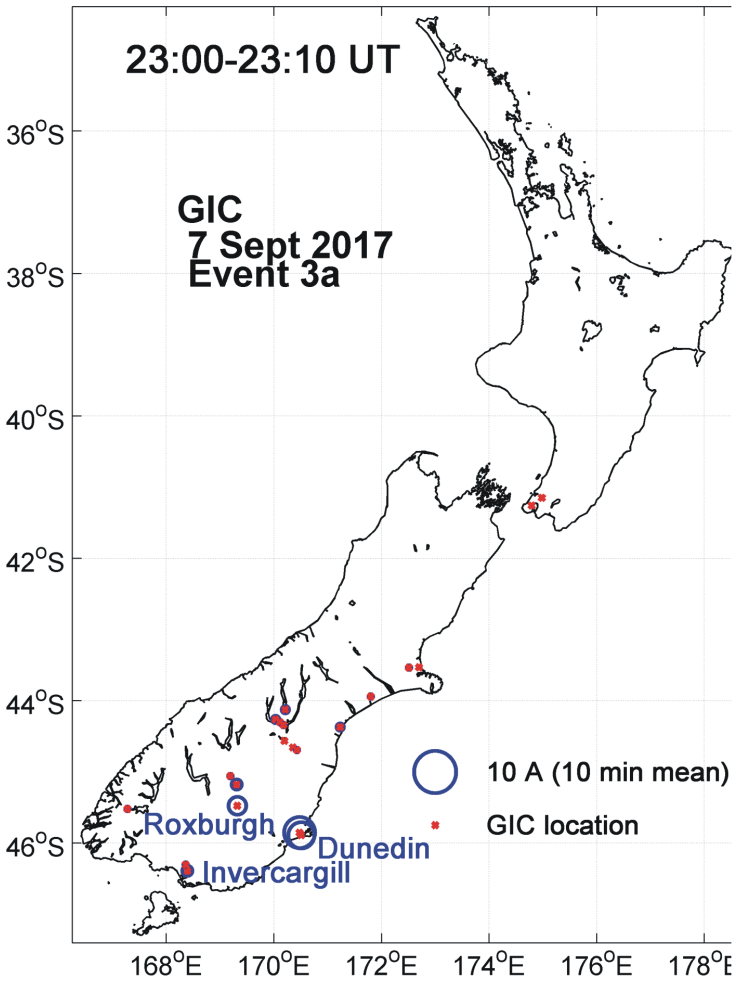
23:00-23:10 UT
GIC
7 Sept 2017
Event 3a
36°S
38°S
40°S
42°S
44°S
46°S
168°E
170°E
172°E
174°E
176°E
178°E
10 A (10 min mean)
GIC location
Roxburgh
Dunedin
Invercargill

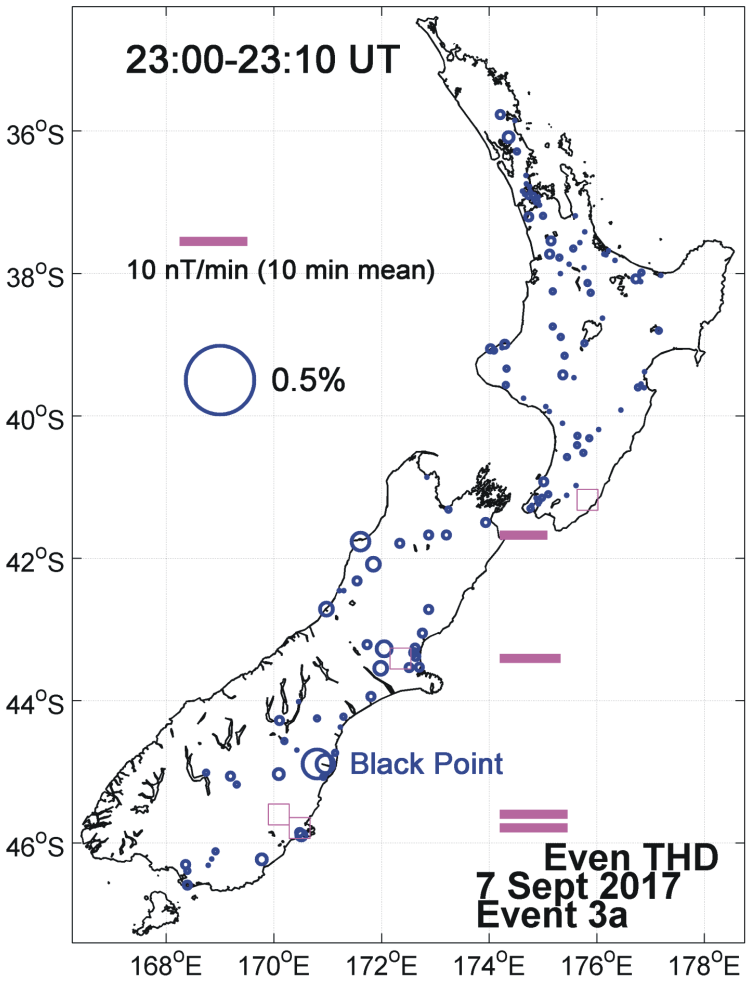
23:00-23:10 UT
10 nT/min (10 min mean)
0.5%
36°S
38°S
40°S
42°S
44°S
46°S
168°E
170°E
172°E
174°E
176°E
178°E
Black Point
Even THD
7 Sept 2017
Event 3a

Figure 6.

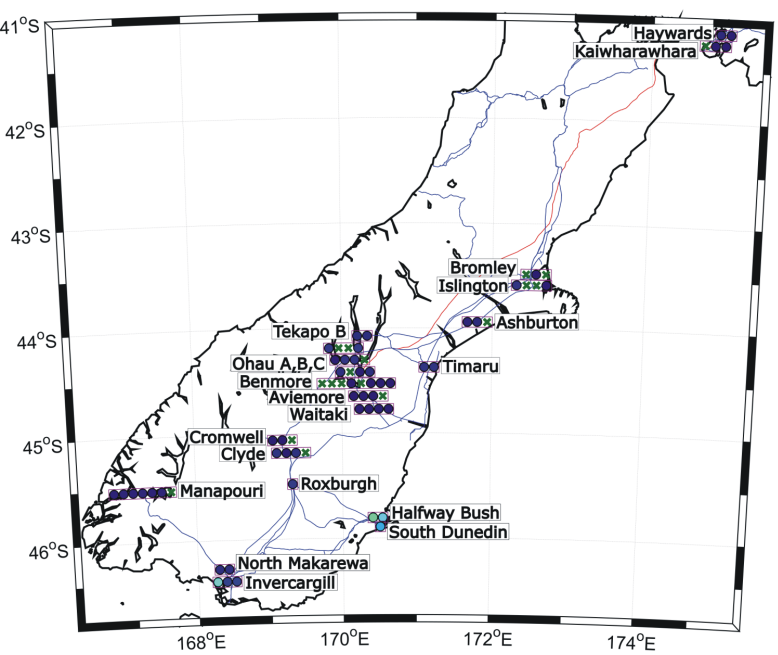
41°S
42°S
43°S
44°S
45°S
46°S
168°E
170°E
172°E
174°E
Haywards
Kaiwharawhara
Bromley
Islington
Ashburton
Tekapo B
Ohau A,B,C
Timaru
Benmore
Aviemore
Waitaki
Cromwell
Clyde
Roxburgh
Manapouri
Halfway Bush
South Dunedin
North Makarewa
Invercargill

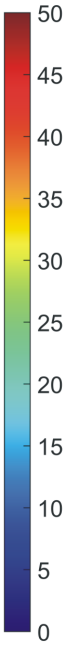
50
45
40
35
30
25
20
15
10
5
0
Current [A]

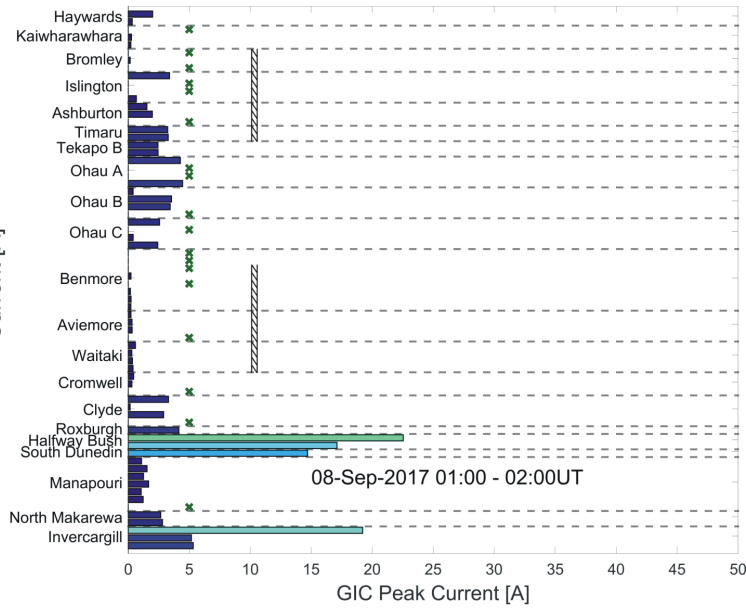
Haywards
Kaiwharawhara
Bromley
Islington
Ashburton
Timaru
Tekapo B
Ohau A
Ohau B
Ohau C
Benmore
Aviemore
Waitaki
Cromwell
Clyde
Roxburgh
Halfway Bush
South Dunedin
Manapouri
North Makarewa
Invercargill
08-Sep-2017 01:00 - 02:00UT
0
5
10
15
20
25
30
35
40
45
50
GIC Peak Current [A]

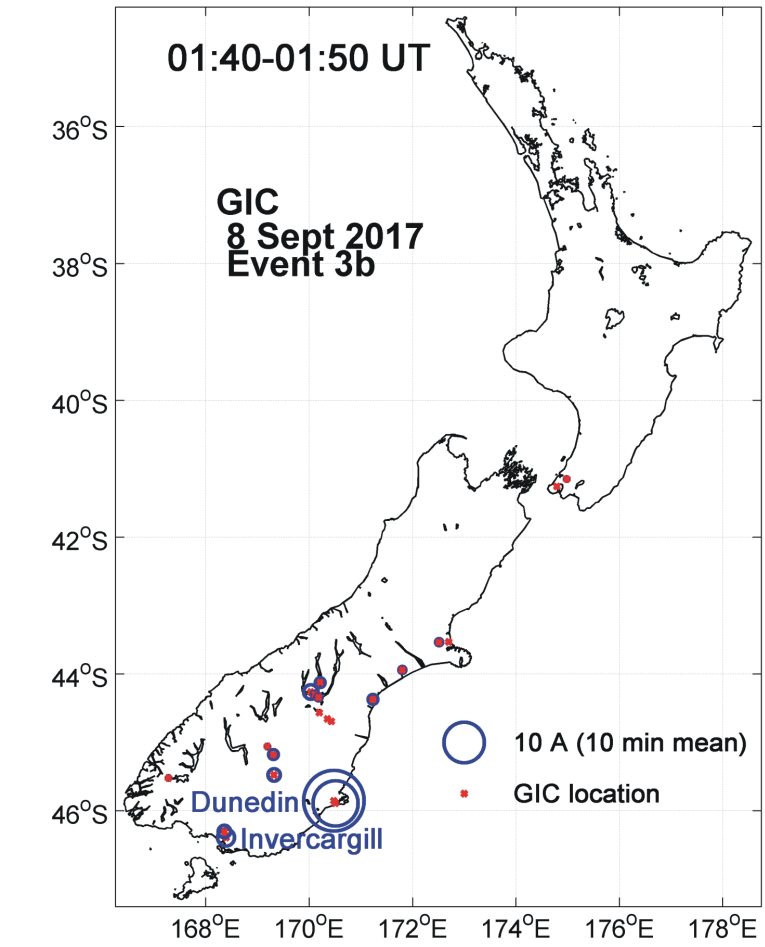
01:40-01:50 UT
GIC
8 Sept 2017
Event 3b
36°S
38°S
40°S
42°S
44°S
46°S
168°E
170°E
172°E
174°E
176°E
178°E
10 A (10 min mean)
GIC location
Dunedin
Invercargill

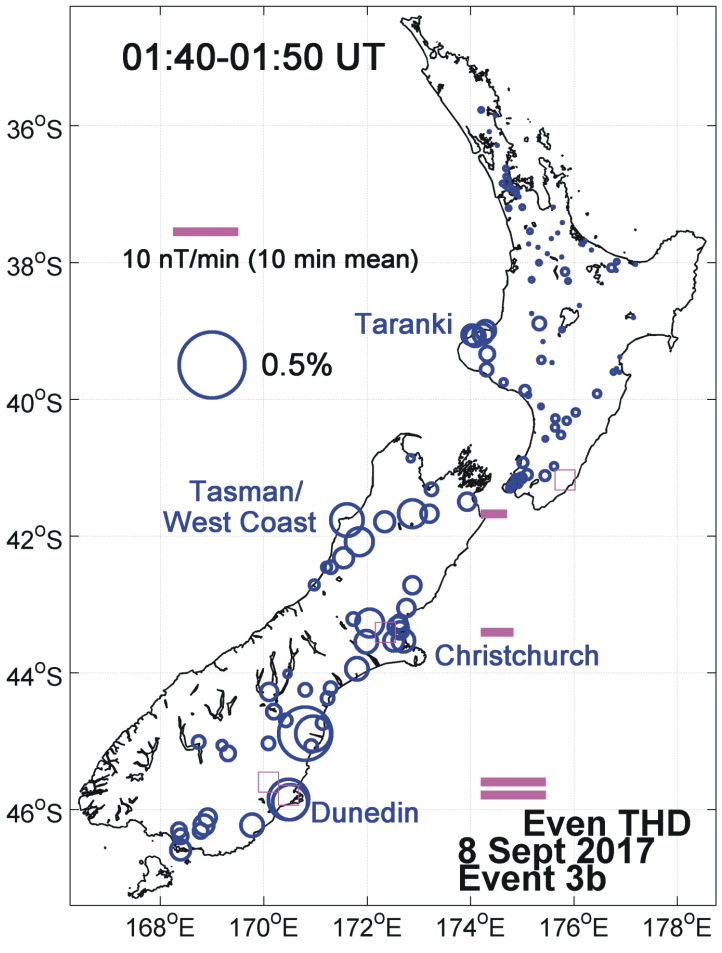
01:40-01:50 UT
36°S
38°S
40°S
42°S
44°S
46°S
168°E
170°E
172°E
174°E
176°E
178°E
10 nT/min (10 min mean)
0.5%
Taranki
Tasman/
West Coast
Christchurch
Dunedin
Even THD
8 Sept 2017
Event 3b

Figure 7.

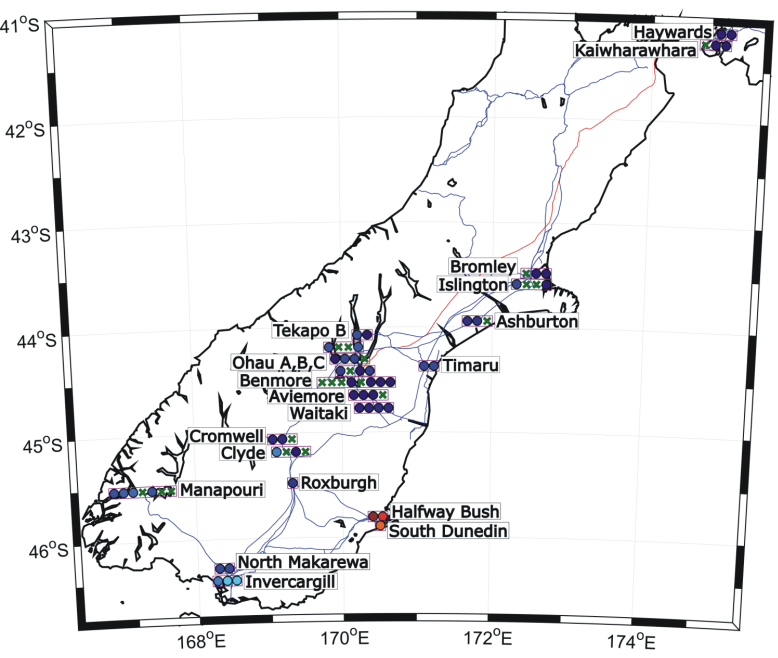
41°S
42°S
43°S
44°S
45°S
46°S
168°E
170°E
172°E
174°E
Haywards
Kaiwharawhara
Bromley
Islington
Ashburton
Tekapo B
Ohau A,B,C
Benmore
Aviemore
Waitaki
Timaru
Cromwell
Clyde
Manapouri
Roxburgh
Halfway Bush
South Dunedin
North Makarewa
Invercargill

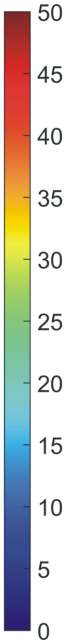
50
45
40
35
30
25
20
15
10
5
0
Current [A]

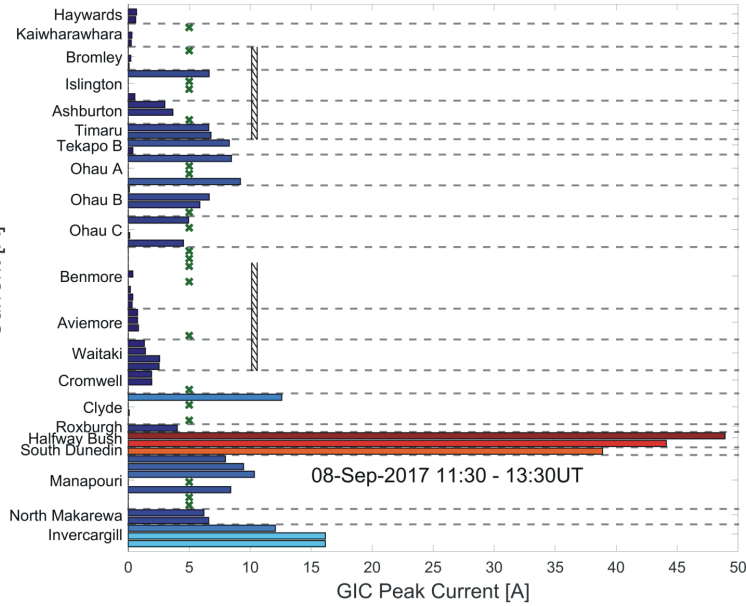
Haywards
Kaiwharawhara
Bromley
Islington
Ashburton
Timaru
Tekapo B
Ohau A
Ohau B
Ohau C
Benmore
Aviemore
Waitaki
Cromwell
Clyde
Roxburgh
Halfway Bush
South Dunedin
Manapouri
North Makarewa
Invercargill
08-Sep-2017 11:30 - 13:30UT
0
5
10
15
20
25
30
35
40
45
50
GIC Peak Current [A]

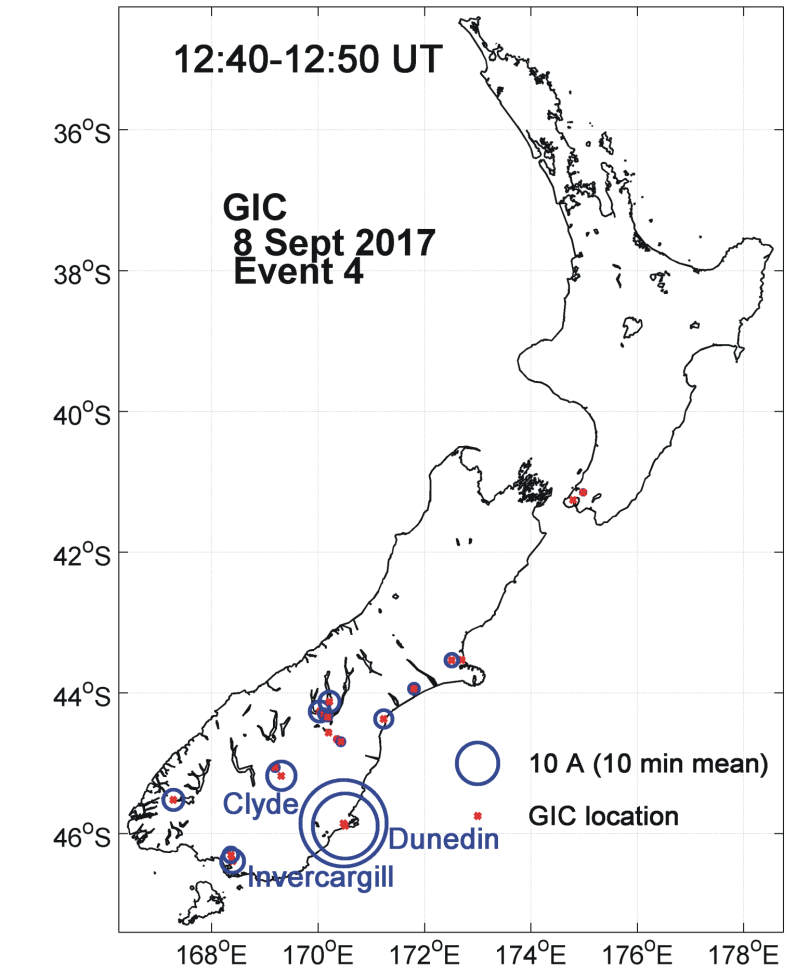
12:40-12:50 UT
GIC
8 Sept 2017
Event 4
36°S
38°S
40°S
42°S
44°S
46°S
168°E
170°E
172°E
174°E
176°E
178°E
10 A (10 min mean)
GIC location
Clyde
Dunedin
Invercargill

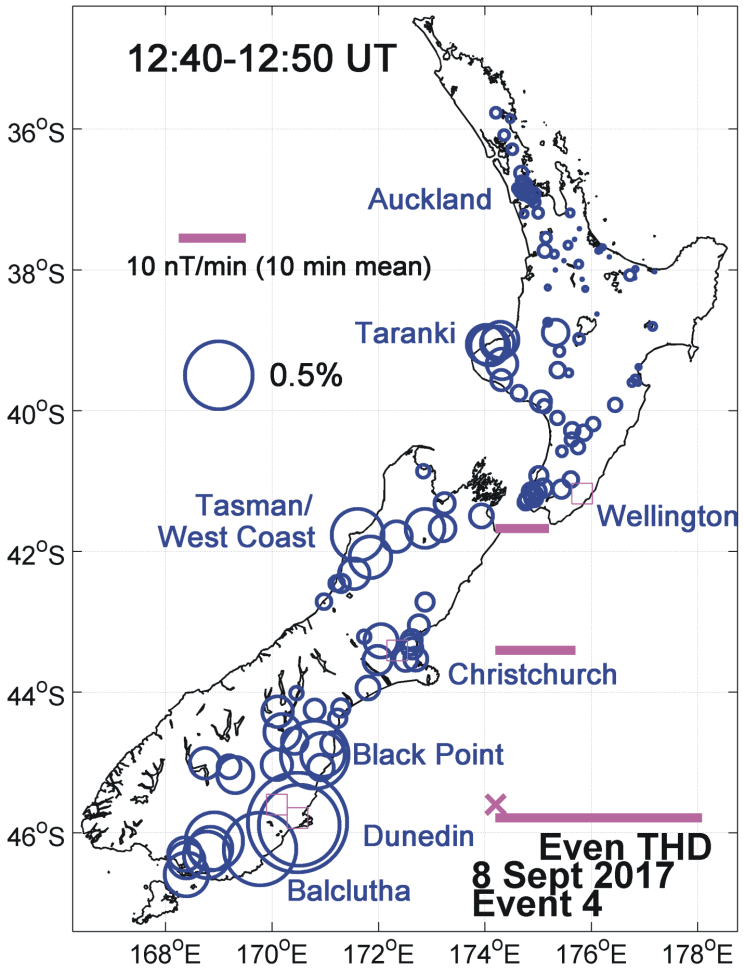
12:40-12:50 UT
36°S
38°S
40°S
42°S
44°S
46°S
168°E
170°E
172°E
174°E
176°E
178°E
Auckland
10 nT/min (10 min mean)
Taranki
0.5%
Tasman/
West Coast
Wellington
Christchurch
Black Point
Dunedin
Balclutha
Even THD
8 Sept 2017
Event 4

Figure 8.

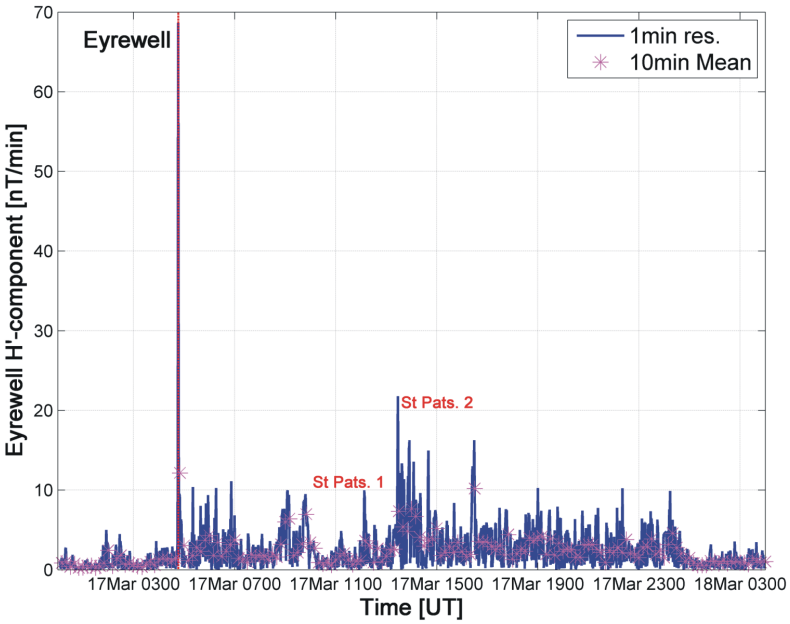
Eyrewell
1min res.
10min Mean
Eyrewell H'-component [nT/min]
St Pats. 1
St Pats. 2
17Mar 0300
17Mar 0700
17Mar 1100
17Mar 1500
17Mar 1900
17Mar 2300
18Mar 0300
Time [UT]

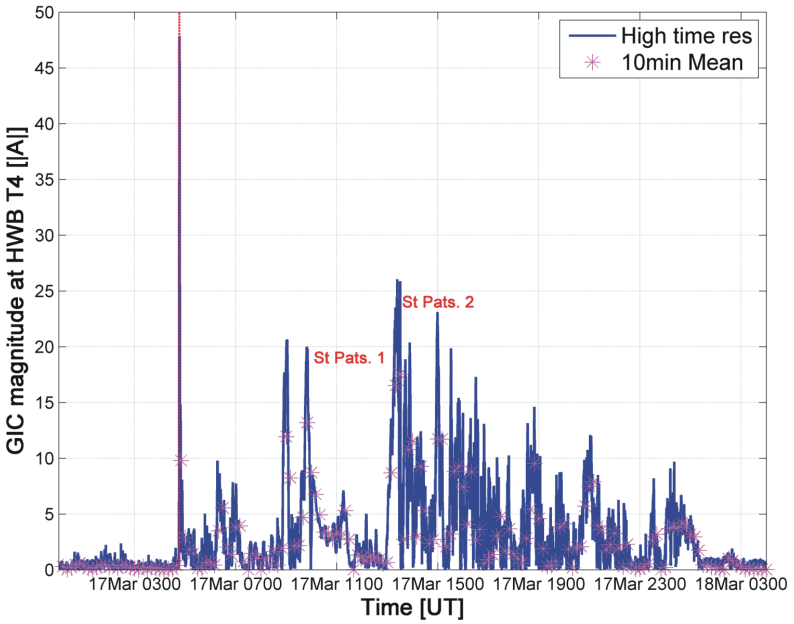
High time res
10min Mean
GIC magnitude at HWB T4 [/A]
St Pats. 1
St Pats. 2
17Mar 0300
17Mar 0700
17Mar 1100
17Mar 1500
17Mar 1900
17Mar 2300
18Mar 0300
Time [UT]

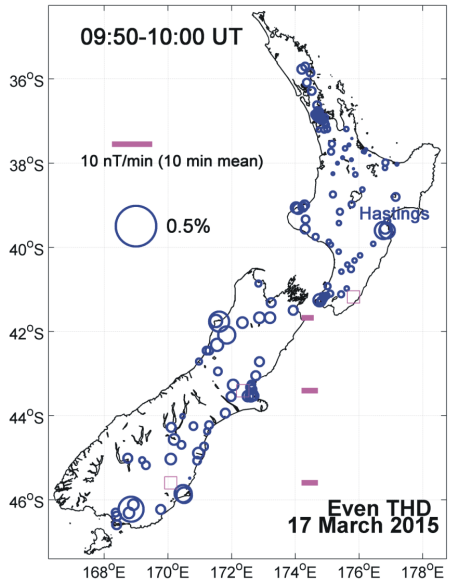
09:50-10:00 UT
10 nT/min (10 min mean)
0.5%
Hastings
Even THD
17 March 2015

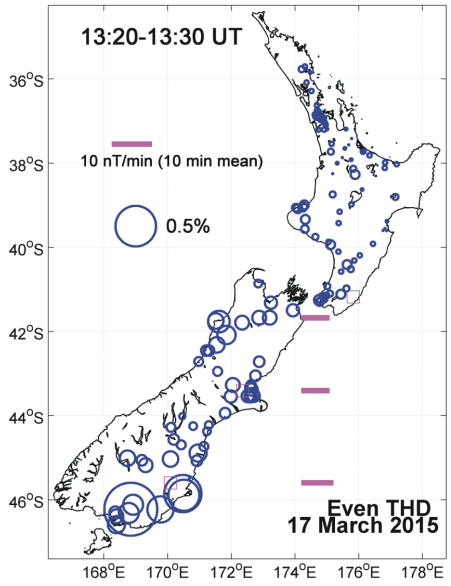
13:20-13:30 UT
10 nT/min (10 min mean)
0.5%
Even THD
17 March 2015